Supporting Information

Dual Lock-and-Key Activated Theranostic for Highly Specific Near-Infrared Imaging and Photodynamic/Chemodynamic Synergistic Therapy of Hepatocellular Carcinoma

Fan Zheng [a,b,‡], Heying Yao [a,b,‡], Duoyang Fan [a,b], Zhiyan Li [a,b], Shuai Huang [a,b], Yanpeng Fang [a,b], Xiang Cheng [a,b], Kun Qian [c], Zhen Cheng [c], Wenbin Zeng [a,b,*]

‡ These authors contributed equally to this work.

[a] Xiangya School of Pharmaceutical Sciences, Central South University, Changsha, 410013, PR China.

[b] Hunan Key Laboratory of Diagnostic and Therapeutic Drug Research for Chronic Diseases, Central South University, Changsha, 410013, PR China.

[c] Shanghai Institute of Materia Medica, Chinese Academy of Sciences, Shanghai, 201203, PR China

* Corresponding author. Prof W Zeng, E-mail: wbzeng@hotmail.com.

Table of Contents

1. Experimental section

1.1 Materials

All chemicals were purchased from commercial suppliers and employed as received. All buffers were prepared using deionized water purified through an ultra-purification system. 2',7'-dichlorodihydrofluorescein diacetate (DCFH-DA), 9',10'-anthracenediyl -bis(methylene)-dimalonic acid (ABDA), 2,2,6,6-tetramethyl -4-piperidone hydrochloride (TEMP), and 5,5-dimethyl -1-pyrroline-N-oxide (DMPO) were purchased from Sigma-Aldrich. Dihydrorhodamine 123 (DHR123), terephthalic acid (TA), and chlorin e6 (Ce6) were purchased from Aladdin Co., Ltd. 3-(4,5-dimethyl -2-thiazolyl) -2,5-diphenyl-2-H-tetrazolium bromide (MTT), Hoechst33342, dihydroethidium (DHE), calcein AM/propidium iodide (PI) detection kit, and lipid peroxidation detection kit C11-BODIPY$^{TM\ 589/591}$ were purchased from Beyotime Biotechnology Co., Ltd. Hydroxyphenyl fluorescein (HPF) was purchased from Maokang Bio. Co., Ltd.

1.2 Apparatus

^{1}H NMR and ^{13}C NMR spectra of all compounds were recorded on a Bruker Advance spectrometer (Rheinstetten, Germany) utilizing tetramethylsilane (TMS) as an internal standard. UV-vis absorption spectra were measured on a UV-2450 UV-visible spectrophotometer (Shimadzu, Japan). Fluorescence spectra were received with a Hitachi F-2700 fluorescence spectrophotometer (Hitachi, Japan). The fluorescence inverted microscope Olympus IX51 and Cytation 5 (BioTek) were used to observe reactive oxygen species (ROS) staining and live/dead cell staining. Confocal laser scanning microscope (CLSM) images were captured using TCS SP8 (Leica, Germany) confocal laser scanning microscope. The MTT assay was carried out with a microplate reader (SpectraMax M2, USA). *In vivo* animals' fluorescence imaging was performed by the S12-IVIS SPERTRUM living imaging system (PerkinElmer).

1.3 Synthesis

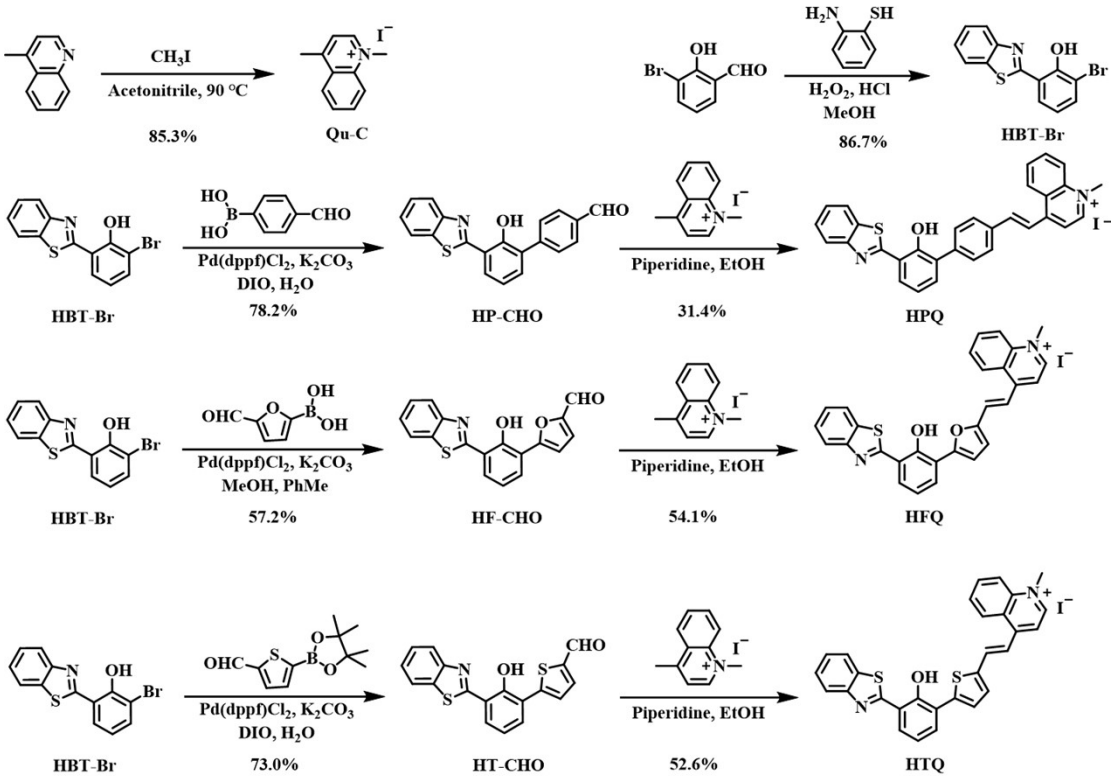

Scheme S1. The synthesis routes of **HPQ**, **HFQ**, and **HTQ**.

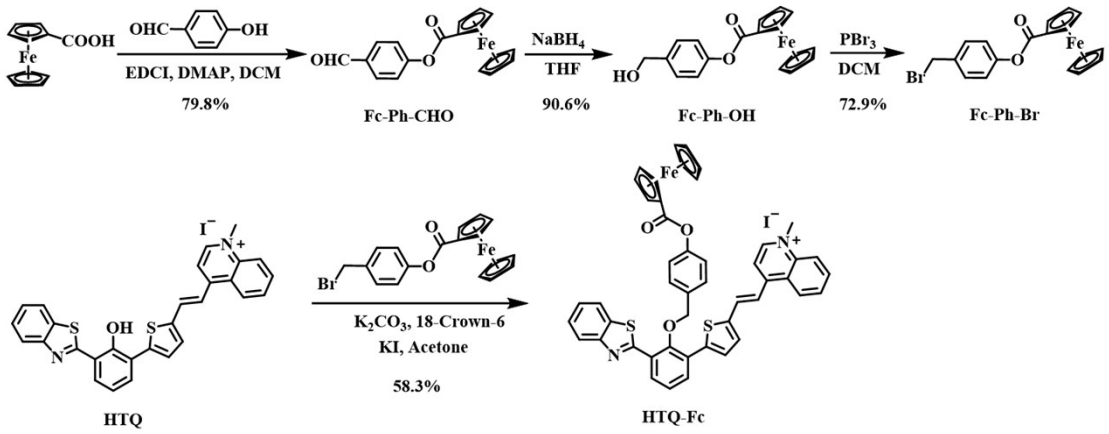

Scheme S2. The synthesis route of **HTQ-Fc**.

Synthesis of compound **Qu-C**.

4-Methylquinoline (715 mg, 5.00 mmol) and iodomethane (374 μL, 6.00 mmol) were dissolved in 8 mL acetonitrile. Then the mixture was heated to 90 °C for 6 h. After the reaction was completed, the solvent was removed under reduced pressure and washed with hexane for three times to give compound **Qu-C** as a yellow solid (1215

mg, yield 85.3%). **^{1}H NMR** (500 MHz, DMSO-d_6) δ 9.38 (d, J = 6.0 Hz, 1H), 8.54 (dd, J = 8.5, 1.4 Hz, 1H), 8.50 (d, J = 8.9 Hz, 1H), 8.28 (ddd, J = 8.5, 7.0, 1.4 Hz, 1H), 8.11-8.04 (m, 2H), 4.59 (s, 3H), 3.01 (s, 3H). **^{13}C NMR** (125 MHz, DMSO-d_6) δ 158.64, 149.45, 138.16, 135.42, 130.13, 128.95, 127.28, 122.95, 120.03, 45.55, 20.12.

Synthesis of compound **HBT-Br**

3-Bromo-2-hydroxybenzaldehyde (201 mg, 1.00 mmol) and 2-aminobenzenethiol (150 mg, 1.20 mmol) were dissolved in 5 mL methanol, stirring at room temperature. A few drops of 30% H_2O_2 and 1 drop of 1 M HCl were added to the bottle dropwise. The reaction mixture was stirred for 6 h. After the reaction was completed, the solvent was removed under reduced pressure and purified by silica column chromatography with hexane/ethyl acetate (100:1, v/v) to give compound **HBT-Br** as a white solid (264 mg, yield: 86.7 %). **^{1}H NMR** (500 MHz, Chloroform-*d*) δ 13.47 (s, 1H), 7.99 (d, J = 8.3 Hz, 1H), 7.92 (d, J = 8.3 Hz, 1H), 7.68 (dd, J = 7.8, 1.5 Hz, 1H), 7.65 (dd, J = 7.8, 1.5 Hz, 1H), 7.54 (ddd, J = 8.3, 7.3, 1.2 Hz, 1H), 7.45 (ddd, J = 8.3, 7.3, 1.2 Hz, 1H), 6.87 (t, J = 7.8 Hz, 1H). **^{13}C NMR** (150 MHz, Chloroform-*d*) δ 168.51, 154.74, 151.35, 135.93, 132.72, 127.49, 127.00, 126.00, 122.36, 121.62, 120.22, 117.73, 111.87.

Synthesis of compound **HP-CHO**

Compound **HBT-Br** (305 mg, 1.00 mmol), 4-formylphenyl boronic acid (225 mg, 1.50 mmol), K_2CO_3 (552 mg, 4.00 mmol), and [1,1'-bis (diphenylphosphino) ferrocene] dichloropalladium (II) (Pd(dppf)Cl_2, 10 mg) were added to a 100 mL three-necked bottle, then vacuumed and protected by N_2. 8 mL of methanol and 5 mL of toluene were added to dissolve the compounds, after vacuuming and protecting by N_2. Finally, the mixture was heated at 90 °C for 6 h. After the reaction was completed, the solvent was removed under reduced pressure and purified by silica column chromatography with hexane/ethyl acetate (50:1, v/v) to give compound **HP-CHO** as a pale-yellow solid (259 mg, yield: 78.2%). **^{1}H NMR** (500 MHz, Chloroform-*d*) δ 13.23 (s, 1H), 10.07 (s, 1H), 7.96 (t, J = 8.7 Hz, 3H), 7.92 (d, J = 8.0 Hz, 1H), 7.86 (d, J = 8.0 Hz, 2H), 7.76 (dd, J = 7.9, 1.6 Hz, 1H), 7.51 (t, J = 7.7 Hz, 1H), 7.47 (dd, J = 7.9, 1.6 Hz, 1H), 7.43 (t, J = 7.6 Hz, 1H), 7.06 (t, J = 7.7 Hz, 1H). **^{13}C NMR** (125 MHz, Chloroform-*d*) δ 192.02, 169.36, 155.34, 151.59, 144.25, 135.20, 133.55, 132.66, 130.12, 129.57,

129.28, 128.70, 126.89, 125.82, 122.21, 121.56, 119.64, 117.32.

Synthesis of compound **HPQ**

Compound **HP-CHO** (165 mg, 0.50 mmol) and compound **Qu-C** (285 mg, 1.00 mmol) were dissolved in 6 mL of EtOH. Piperidine (20 μL) was added dropwise, and then the mixture was reacted at 90 °C for 6 h. After the reaction was completed, the solvent was removed under reduced pressure and the residue was purified by silica column chromatography with dichloromethane/methanol (40:1, v/v) to give compound **HPQ** as an orange-yellow solid (94 mg, yield: 31.4%). **^{1}H NMR** (600 MHz, DMSO-d_6) δ 13.00 (s, 1H), 9.38 (d, J = 6.5 Hz, 1H), 9.07 (d, J = 8.5 Hz, 1H), 8.54 (d, J = 6.5 Hz, 1H), 8.45 (d, J = 8.9 Hz, 1H), 8.37 (d, J = 15.9 Hz, 1H), 8.29-8.25 (m, 1H), 8.25-8.20 (m, 2H), 8.11-8.08 (m, 3H), 8.07-8.04 (m, 1H), 7.90 (d, J = 8.9 Hz, 1H), 7.83 (d, J = 8.5 Hz, 2H), 7.61 (ddd, J = 16.7, 7.6, 1.4 Hz, 2H), 7.53 (t, J = 7.6 Hz, 1H), 7.17 (t, J = 7.6 Hz, 1H), 4.57 (s, 3H). **^{13}C NMR** (150 MHz, DMSO-d_6) δ 169.50, 154.89, 152.92, 151.35, 148.52, 142.97, 139.96, 139.16, 135.46, 134.89, 134.24, 132.79, 130.29, 129.75, 129.38, 129.17, 129.05, 127.64, 126.96, 126.80, 126.54, 122.89, 122.41, 120.76, 120.27, 119.80, 117.29, 116.79, 45.23. **HRMS**: m/z calcd for $C_{31}H_{23}N_2OS^+$([M]$^+$) 471.1526, found 471.1526.

Synthesis of compound **HF-CHO**

Compound **HBT-Br** (264 mg, 0.87 mmol), 5-formylthiophen-2-boronic acid (203 mg, 1.3 mmol), K_2CO_3 (179 mg, 1.3 mmol), and Pd(dppf)Cl_2 (10 mg) were added to a 100 mL three-necked bottle, then vacuumed and protected by N_2. 8 mL of methanol and 5 mL of toluene were added to dissolve the compounds, after vacuuming and protecting by N_2. Finally, the mixture was heated at 90 °C for 6 h. After the reaction was completed, the solvent was removed under reduced pressure and purified by silica column chromatograph with hexane/ethyl acetate (40:1, v/v) to give compound **HF-CHO** as a pale-yellow solid (159 mg, yield: 57.2%). **^{1}H NMR** (500 MHz, Chloroform-*d*) δ 13.74 (s, 1H), 9.68 (s, 1H), 8.17 (dd, J = 7.8, 1.6 Hz, 1H), 8.04 (dd, J = 8.1, 1.1 Hz, 1H), 7.95 (d, J = 8.1 Hz, 1H), 7.77 (dd, J = 7.8, 1.6 Hz, 1H), 7.58-7.54 (m, 1H), 7.48-7.45 (m, 2H), 7.40 (d, J = 3.8 Hz, 1H), 7.10 (t, J = 7.8 Hz, 1H). **^{13}C NMR** (100 MHz, Chloroform-*d*) δ 177.23, 169.13, 155.64, 151.43, 151.30, 150.96, 132.53, 130.08,

129.29, 129.22, 126.96, 125.94, 122.19, 121.63, 119.60, 118.25, 117.34, 113.18.

Synthesis of compound **HFQ**

Compound **HF-CHO** (159 mg, 0.50 mmol) and compound **Qu-C** (285 mg, 1.00 mmol) were dissolved in 6 mL of EtOH. Piperidine (20 μL) was added dropwise, and then the mixture was reacted at 90 °C for 6 h. After the reaction was completed, the solvent was removed under reduced pressure and the residue was purified by silica column chromatography with dichloromethane/methanol (30:1, v/v) to give compound **HFQ** as an amaranth solid (159 mg, yield: 54.1%). **^{1}H NMR** (500 MHz, DMSO-d_6) δ 13.56 (s, 1H), 9.23 (d, J = 6.6 Hz, 1H), 8.94 (d, J = 8.4 Hz, 1H), 8.38 (dd, J = 11.8, 7.7 Hz, 2H), 8.32 (dd, J = 7.7, 1.3 Hz, 1H), 8.26-8.22 (m, 1H), 8.19 (d, J = 7.8 Hz, 1H), 8.09-8.02 (m, 4H), 7.87 (dd, J = 7.7, 1.3 Hz, 1H), 7.62-7.57 (m, 1H), 7.55-7.50 (m, 1H), 7.39 (d, J = 3.6 Hz, 1H), 7.26 (d, J = 3.6 Hz, 1H), 7.23 (d, J = 7.8 Hz, 1H), 4.46 (s, 3H). **^{13}C NMR** (125 MHz, DMSO-d_6) δ 169.40, 154.52, 152.92, 152.21, 151.22, 151.16, 148.02, 139.15, 135.41, 135.38, 132.58, 129.95, 129.66, 129.30, 129.22, 127.72, 126.65, 126.44, 122.89, 122.38, 120.73, 120.39, 119.67, 118.57, 117.22, 117.02, 115.83, 114.72, 44.95. **HRMS**: m/z calcd for $C_{29}H_{21}N_2O_2S^+$([M]$^+$) 461.1318, found 461.1317.

Synthesis of compound **HT-CHO**

Compound **HBT-Br** (305 mg, 1.00 mmol), 5-(4,4,5,5-tetramethyl-1,3,2-dioxaborolan-2-yl)thiophene-2-carbaldehyde (357 mg, 1.50 mmol), K_2CO_3 (552 mg, 4 mmol), and Pd(dppf)Cl_2 (10 mg) were added to a 100 mL three-necked bottle, then vacuumed and protected by N_2. 8 mL of methanol and 5 mL of toluene were added to dissolve the compounds, after vacuuming and protecting by N_2. Finally, the mixture was heated at 90 °C for 6 h. After the reaction was completed, the solvent was removed under reduced pressure and purified by silica column chromatograph with hexane/ethyl acetate (30:1, v/v) to give Compound **HT-CHO** as a pale-yellow solid (246 mg, yield: 73%). **^{1}H NMR** (500 MHz, Chloroform-*d*) δ 13.85 (s, 1H), 9.95 (s, 1H), 8.03 (d, J = 8.2 Hz, 1H), 7.93 (d, J = 8.2 Hz, 1H), 7.82 (d, J = 7.8 Hz, 1H), 7.79 (d, J = 1.3 Hz, 2H), 7.75 (d, J = 7.8 Hz, 1H), 7.55 (t, J = 7.7 Hz, 1H), 7.45 (t, J = 7.7 Hz, 1H), 7.05 (t, J = 7.8 Hz, 1H). **^{13}C NMR** (125 MHz, Chloroform-*d*) δ 183.09, 169.05, 155.18, 151.42,

148.96, 142.69, 136.15, 132.59, 131.44, 129.08, 127.01, 126.69, 125.99, 122.30, 122.12, 121.59, 119.62, 117.66.

Synthesis of compound **HTQ**

Compound **HT-CHO** (168 mg, 0.50 mmol) and compound **Qu-C** (285 mg, 1.00 mmol) were dissolved in 6 mL of EtOH. Piperidine (20 μL) was added dropwise, and then the mixture was reacted at 90 °C for 6 h. After the reaction was completed, the solvent was removed under reduced pressure and the residue was purified by silica column chromatography with dichloromethane/methanol (30:1, v/v) to give compound **HTQ** as an amaranth solid (159 mg, yield: 52.6%). **^{1}H NMR** (500 MHz, DMSO-d_6) δ 13.88 (s, 1H), 9.28 (d, J = 6.6 Hz, 1H), 8.97 (d, J = 8.4 Hz, 1H), 8.42 (dd, J = 14.4, 6.6 Hz, 3H), 8.26-8.22 (m, 2H), 8.16 (d, J = 8.4 Hz, 1H), 8.10-8.07 (m, 1H), 8.05-7.99 (m, 2H), 7.92 (t, J = 5.9 Hz, 2H), 7.82 (d, J = 4.0 Hz, 1H), 7.64 (t, J = 7.8 Hz, 1H), 7.56 (t, J = 7.8 Hz, 1H), 7.19 (t, J = 7.6 Hz, 1H), 4.52 (s, 3H). **^{13}C NMR** (125 MHz, DMSO-d_6) δ 169.51, 152.52, 151.13, 148.12, 141.44, 139.22, 136.45, 136.43, 135.38, 132.73, 132.67, 131.37, 131.34, 129.64, 129.22, 127.81, 127.69, 126.75, 126.73, 126.43, 123.02, 122.43, 122.31, 120.89, 119.74, 118.10, 117.51, 115.97, 45.00. **HRMS**: m/z calcd for $C_{29}H_{21}N_2OS_2^+$ ($[M]^+$) 477.1090, found 477.1095.

Synthesis of **Fc-Ph-CHO**

Ferrocenecarboxylic acid (230 mg, 1.00 mmol), 4-hydroxybenzaldehyde (122 mg, 1.00 mmol), and 4-dimethylaminopyridine (10 mg) were dissolved in 8 mL of anhydrous DCM. Then the mixture was stirred at 0 °C. 1-(3-dimethylaminopropyl) -3-ethylcarbodiimide (EDC, 310 μL, 2.00 mmol) was added to the mixture dropwise. The mixture was reacted at room temperature for 1 h. After the reaction was completed, the solvent was removed under reduced pressure and purified by silica column chromatography with hexane/ethyl acetate (30:1, v/v) to give compound **Fc-Ph-CHO** as an orange solid (266 mg, yield: 79.8%). **^{1}H NMR** (600 MHz, Chloroform-*d*) δ 10.02 (s, 1H), 7.96 (d, J = 8.3 Hz, 2H), 7.37 (d, J = 8.3 Hz, 2H), 4.98 (t, J = 1.9 Hz, 2H), 4.55 (t, J = 1.9 Hz, 2H), 4.32 (s, 5H). **^{13}C NMR** (125 MHz, Chloroform-*d*) δ 191.00, 169.80, 155.77, 133.81, 131.28, 122.47, 72.32, 70.74, 70.07, 69.33.

Synthesis of **Fc-Ph-OH**

Compound **Fc-Ph-CHO** (266 mg, 0.80 mmol) was dissolved in anhydrous THF, and $NaBH_4$ (30 mg, 0.80 mmol) was added to the mixture in batches. The mixture was reacted at room temperature for 2 h. After the reaction was completed, the solvent was removed under reduced pressure and purified by silica column chromatography with hexane/ethyl acetate (3:1, v/v) to give compound **Fc-Ph-OH** as an orange oily liquid (243 mg, yield: 90.6%). **^{1}H NMR** (500 MHz, Chloroform-*d*) δ 7.41 (d, *J* = 8.2 Hz, 2H), 7.16 (d, *J* = 8.2 Hz, 2H), 4.97 (t, *J* = 1.9 Hz, 2H), 4.70 (s, 2H), 4.51 (t, *J* = 1.9 Hz, 2H), 4.31 (s, 5H). **^{13}C NMR** (125 MHz, Chloroform-*d*) δ 170.58, 150.25, 138.43, 128.11, 121.80, 72.04, 70.69, 70.02, 69.98, 64.68.

Synthesis of **Fc-Ph-Br**

Compound **Fc-Ph-OH** (243 mg, 0.72 mmol) was dissolved in anhydrous DCM and stirred at 0 °C. Then phosphorus tribromide (137 μL, 1.44 mmol) was added to the mixture dropwise. The mixture was reacted at room temperature for 1 h. After the reaction was completed, pour the mixture into ice. Adjust its pH with $NaHCO_3$ solution to around 7. Extract the reaction mixture with DCM. The combined organic layer was dried over anhydrous magnesium sulfate, filtered and concentrated by rotary evaporation under reduced pressure. It was further purified by silica column chromatography with hexane/ethyl acetate (30:1, v/v) to give compound **Fc-Ph-Br** as an orange solid (209 mg, yield: 72.9%). **^{1}H NMR** (500 MHz, Chloroform-*d*) δ 7.48 (d, *J* = 8.5 Hz, 2H), 7.20 (d, *J* = 8.5 Hz, 2H), 4.99 (t, *J* = 2.0 Hz, 2H), 4.55 (s, 2H), 4.54 (t, *J* = 2.0 Hz, 2H), 4.33 (s, 5H). **^{13}C NMR** (125 MHz, Chloroform-*d*) δ 170.17, 150.88, 135.10, 130.26, 122.09, 72.06, 70.68, 70.00, 69.86. **HRMS**: m/z calcd for $C_{18}H_{15}BrFeO_2$([M + H]$^+$) 398.9605, found 398.9653.

Synthesis of **HTQ-Fc**

Compound **HTQ** (159 mg, 0.26 mmol), compound **Fc-Ph-Br** (207 mg, 0.52 mmol), K_2CO_3 (72 mg, 0.52 mmol), 18-crown-6 (137 mg, 0.52 mmol), and KI (432 mg, 2.60 mmol) were dissolved in 6 mL of acetone. Then the solution was vacuumed and protected by N_2. The mixture was stirred at 60 °C for 8 h. Subsequently, the mixture was extracted with DCM, and the organic phase was dried over anhydrous Na_2SO_4. After removing the solvent under reduced pressure, the residue was purified by silica

column chromatography with dichloromethane/methanol (30:1, v/v) to give compound **HTQ-Fc** as a dark red solid (140 mg, yield: 58.3%). **^{1}H NMR** (500 MHz, DMSO-d_6) δ 9.34 (d, J = 6.5 Hz, 1H), 8.88 (d, J = 8.4 Hz, 1H), 8.50 (d, J = 6.5 Hz, 1H), 8.46 (d, J = 9.4 Hz, 1H), 8.43 (d, J = 2.7 Hz, 1H), 8.39 (dd, J = 7.7, 1.6 Hz, 1H), 8.26 (t, J = 7.9 Hz, 1H), 8.17 (d, J = 7.9 Hz, 1H), 8.13 (d, J = 8.1 Hz, 1H), 8.07 (t, J = 7.7 Hz, 1H), 8.01-7.95 (m, 2H), 7.86 (d, J = 4.0 Hz, 1H), 7.79 (d, J = 4.0 Hz, 1H), 7.61 - 7.48 (m, 5H), 7.21 (d, J = 8.4 Hz, 2H), 4.91 (s, 2H), 4.85 (t, J = 1.9 Hz, 2H), 4.61 (t, J = 1.9 Hz, 2H), 4.53 (s, 3H), 4.29 (s, 5H). **^{13}C NMR** (125 MHz, DMSO-d_6) δ 170.00, 162.40, 153.52, 152.41, 152.28, 150.71, 148.34, 142.20, 142.17, 139.22, 136.02, 135.95, 135.42, 133.96, 132.83, 132.77, 132.75, 132.72, 130.54, 130.11, 129.77, 129.59, 129.31, 128.86, 128.43, 127.07, 126.50, 126.39, 126.09, 123.38, 122.63, 122.19, 119.90, 118.94, 116.41, 78.22, 72.65, 70.69, 70.25, 69.74, 45.17. **HRMS**: m/z calcd for $C_{47}H_{35}FeN_2O_3S_2^+$([M]$^+$) 795.1433, found 795.1442.

1.4 General procedure for the detection of viscosity

HPQ, **HFQ**, **HTQ**, and **HTQ-Fc** were dissolved in DMSO to afford 5 mM stock solution. Deionized water and glycerin were mixed with different proportions to obtain different viscosity solutions. The viscosity values of each mixed solution were measured using viscosimeter (NDJ-8S) as 1.71, 2.45, 3.55, 5.61, 14, 18.5, 42.9, 59.2, 105, 184, and 480 cp. After the addition of the probe (10 μM) to different viscous solutions, the fluorescence spectra were measured to investigate the corresponding viscosity response ability.

1.5 Anti-interference study of viscosity

In the anti-interference study, various competitive physiologically relevant analytes, including $Zn(OAc)_2$, $FeSO_4$, $CoCl_2$, $CaCl_2$, $MgSO_4$, $AlCl_3$, NaBr, NaI, KNO_3, $NaNO_2$, Na_2SO_3, glucose, galactose, H_2O_2, valine, glycine, proline, cysteine, and glutamic acid were prepared as the concentration of 100 μM. The concentration of **HPQ**, **HFQ**, and **HTQ** was 10 μM. The fluorescence spectra were measured in water or water/glycerin (5/5, v/ v) solutions.

1.6 Total ROS detection

2',7'-dichlorodihydrofluorescein (DCFH) was utilized as the indicator to detect

the total ROS generation capacity of the photosensitizers. 50 μM DCFH was mixed with the photosensitizer (such as **HPQ**, **HFQ**, **HTQ**, **HTQ-Fc**, or Ce6) in PBS. The fluorescence of different solutions was measured after white light irradiation (60 mW cm^{-2}) at different time intervals (λ_{ex} = 460 nm). The ratio of the fluorescence intensity at different time points to the initial intensity (I/I_0) was applied to reveal the total ROS production rate (λ_{em} = 525 nm).

1.7 Singlet oxygen ($^1O_2$) detection

To detect the generation of $^1O_2$, 9,10-anthracenediyl-bis(methylene) dimalonic acid (ABDA) was applied as the indicator. The stock solution of ABDA (5 mM) was prepared in DMSO. Before the test, 990 μL PBS, 10 μL ABDA, and other substances were mixed thoroughly. Then the absorbance of ABDA at 378 nm was recorded after white light irradiation (60 mW cm^{-2}) at different times. The $^1O_2$ generation rate was basically characterized by the ratio of the absorbance at 378 nm after light irradiation to the initial absorbance (A/A_0).

1.8 Superoxide radical ($O_2^{\bullet-}$) detection

Dihydrorhodamine 123 (DHR123) was used as the indicator to detect the $O_2^{\bullet-}$ generation. 5 μM DHR123 was mixed with the photosensitizer (such as **HPQ**, **HFQ**, **HTQ**, **HTQ-Fc**, or Ce6) in PBS. The fluorescence of different solutions was measured after white light irradiation (60 mW cm^{-2}) at different time intervals (λ_{ex} = 488 nm). The ratio of the fluorescence intensity at different time points to the initial intensity (I/I_0) was applied to indicate the $O_2^{\bullet-}$ generation rate (λ_{em} = 526 nm).

1.9 Hydroxyl radical (•OH) detection by TA

Terephthalic acid (TA) was utilized as an indicator to detect the •OH generation. 5 mM TA was mixed with the photosensitizer (such as **HPQ**, **HFQ**, **HTQ**, **HTQ-Fc**, or Ce6) in PBS. The fluorescence of different solutions was measured after white light irradiation (60 mW cm^{-2}) at different time intervals (λ_{ex} = 315 nm). The ratio of the fluorescence intensity at different time points to the initial intensity (I/I_0) was used to indicate the •OH generation rate (λ_{em} = 445 nm).

1.10 General procedure for CE detection

The stock solution of **HTQ-Fc** (5 mM) was prepared in DMSO. Unless otherwise specified, all the tests related to CE response were performed in a water/glycerin mixture solution with a viscosity value of 42.9 cp. Before the test, 2 μL **HTQ-Fc** stock solution was added to the solution, and then an appropriate volume of CE was added to the solution to obtain CE with different concentrations of 0.1, 0.2, 0.3, 0.4, 0.6, 0.8, 1.0, 1.5, and 2.0 U/mL. After incubation at 37 ℃ for 1 h, the fluorescence spectra were measured to investigate the relationship between **HTQ-Fc** and CE.

1.11 Anti-interference study of CE

In the anti-interference study, various competitive physiologically relevant ions and amino acid derivatives, including $AlCl_3$, $FeSO_4$, $CaCl_2$, $MgSO_4$, $CoCl_2$, NaF, NaBr, NaI, KNO_3, K_2CO_3, Na_2S, NaHS, tyrosine, proline, glycine, glutamic acid, and leucine, were prepared as the concentration of 100 μM. Various competitive enzymes, including aminopeptidase N, γ-glutamyl transferase, nitroreductase, tyrosinase, β-galactosidase, glucose oxidase, AchE, and BchE, were prepared as the concentration of 2 U/mL. The concentration of CE was prepared as 2 U/mL.

An appropriate volume of CE or other substances was added to the **HTQ-Fc** solution (10 μM) instantly to meet the above concentrations. After incubation at 37 ℃ for 1 h, the fluorescence spectra were measured.

1.12 Inhibition experiments of CE

In the **HTQ-Fc** solution (10 μM) with or without 2.0 U/mL CE, varying concentrations of the CE inhibitor BNPP (0, 0.1, 1, 10, and 100 μM) were added respectively. After incubation at 37 ℃ for 1 h, the fluorescence was measured to investigate the response profile of **HTQ-Fc** to CE activity in the presence of different BNPP concentrations.

1.13 Hydroxyl radical (•OH) detection by TMB

The Fenton catalytic performance was monitored through a 3,3’,5,5’-tetramethyl-[1,1’-biphenyl]-4,4’-diamine (TMB) color test. For example, 2 μL **HTQ-Fc** (5 mM) was mixed thoroughly with a PBS solution containing 20 μL TMB (25 mM) and 2 μL

H_2O_2 (125 mM). After incubation at 37 ℃ for different times, the absorbance at 652 nm was measured by a microplate reader.

1.14 Electron spin resonance (ESR) analysis

The types of the produced ROS were confirmed by ESR analysis. 2,2,6,6-tetramethyl-4-piperidone (TEMP) was applied as the $^1O_2$ trapping agent and 5,5-dimethyl-1-pyrroline-N-oxide (DMPO) was employed as the spin trapper for identifying $O_2^{\bullet-}$ and •OH, respectively.

1.15 Cytotoxicity of HTQ or HTQ-Fc in living cells

HSC-T6 cells or Hepa1-6 cells were seeded into 96-well plates at a density of 5×10^3 cells/well with Dulbecco's modified eagle medium (DMEM) containing 10% fetal bovine serum (FBS) and 1% penicillin-streptomycin. All cell cultures were performed in an atmosphere of 5% CO_2 and 95% air at 37 °C unless otherwise noted. After cell adherence to the plate, the original media was replaced by various concentrations of probes. After incubation for 24 h, the media containing **HTQ** or **HTQ-Fc** was replaced by MTT solution (0.5 mg/mL, 100 μL/well) for 4 h. Then, DMSO (150 μL/well) was utilized to replace and the absorption at 490 nm was measured by a microplate reader. The cell viability (%) = $[(OD_{sample} - OD_{blank}) / (OD_{control} - OD_{blank})] \times 100\%$.

To evaluate the photodynamic efficacy of **HTQ** or **HTQ-Fc**, Hepa1-6 cells were seeded in 96-well plates at a density of 5×10^3 cells/well and allowed to finish cell adherence. Cells were then treated with varying concentrations of the probes for 4 h. After replacing the original medium with fresh culture medium, the cells were exposed to white light irradiation (60 mW cm^{-2}) for 15 min. Following an additional 20 h of incubation, cell viability was assessed using the MTT assay.

As in hypoxic conditions (1% O_2, 5% CO_2, 94% N_2), Hepa1-6 cells were transferred to a hypoxic incubator for 6 h before incubation with the probes. Other procedures were similar to normoxic conditions except that cells were incubated in hypoxia.

1.16 Confocal laser scanning microscope (CLSM) imaging

For CLSM imaging, cells were cultured in 35 mm confocal dishes until full adherence was achieved.

For the imaging of intracellular viscosity, HeLa cells were pretreated with either monensin (10 μM) or nystatin (10 μM) for 30 min, and then incubated with 10 μM **HTQ** or **HTQ-Fc** for 30 min, followed by three times washing with PBS buffer (pH = 7.4). Fluorescence images were then taken by a confocal laser scanning microscope (TCS SP8, Leica, with a 60 × objective lens). For the hypertonic and hypotonic group, HeLa cells were incubated with the probe for 30 min, and then were treated with an equal volume of the unsaline HANKS buffer (140 mM NaCl, 2.5 mM KCl, 0.5 mM $MgCl_2$, 1.2 mM $CaCl_2$, 5 mM glucose, 10 mM HEPES pH 7.5) for 10 min before taking CLSM images. Subsequently, 1.33 times the volume of saline HANKS buffer (500 mM NaCl) was added. Fluorescence images were taken after incubation for 5 min.

For the imaging of intracellular CE, Hepa1-6 or HepG2 cells were incubated with 10 μM **HTQ-Fc** for different periods and then washed with PBS for three times. Fluorescence images were then taken by a confocal laser scanning microscope (TCS SP8, Leica, with a 60 × objective lens).

To investigate the specific imaging ability of **HTQ-Fc** at cellular levels, different kinds of cells (including HSC-T6, HEK293T, HeLa, 4T1, Hepa1-6, and HepG2 cells) were incubated with 10 μM **HTQ-Fc** for 30 min or 4 h and then washed with PBS for three times. Fluorescence images were then taken by a confocal laser scanning microscope (TCS SP8, Leica, with a 60 × objective lens).

1.17 Wound healing assay

Hepa1-6 cells were cultured in 6-well plates until they reached approximately 90% confluence. A standardized wound was created in each well using sterile 200 μL pipette tips to generate perpendicular scratches. Wash each well carefully to remove the scratched cells using a serum-free culture medium. Then, the cross lines were photographed by Cytation 5 (BioTek). The cells were maintained in 1% FBS culture medium with or without **HTQ-Fc** (10 μM) for 4 h. For the irradiation group, the plate was exposed to white light irradiation (60 mW cm^{-2}) for 15 min. After further

incubation for 20 h in 1% FBS culture medium, the cross lines were photographed again.

1.18 ROS generation in living cells

DCFH-DA, DHE, and HPF were used to detect the content of total ROS, $O_2^{\bullet-}$, and •OH, respectively. Hepa1-6 cells were seeded into 12-well plates and allowed to finish cell adherence. The media were then replaced with fresh culture media containing 10 μM **HTQ-Fc** and incubated for different time. After that, the cells were incubated with fresh media containing 5 μM DCFH-DA, 10 μM DHE, or 10 μM HPF at 37 °C for 30 min. After washing with PBS, the cells treated with DCFH-DA or DHE were exposed to white light irradiation (60 mW cm^{-2}) for 15 min. The fluorescence images were taken immediately by the fluorescence inverted microscope.

1.19 Calcein AM/PI staining

Calcein AM and PI were used as indicators to detect the distribution of living and dead cells, respectively. Hepa1-6 cells were seeded into 12-well plates and allowed to finish cell adherence. The media were then replaced with fresh culture media containing 10 μM **HTQ-Fc** or **HTQ** and incubated for different time. After washing with PBS, the cells were irradiated with white light (60 mW cm^{-2}) for 15 min, followed by 30 min incubation at 37 °C. Then, the cells were incubated with PBS containing 2 μM Calcein-AM and 2 μM PI at 37 °C for 30 min. The fluorescence images were taken immediately by the fluorescence inverted microscope.

Hepa1-6 cells were seeded into 12-well plates allowed to finish cell adherence. The plates were transferred to a hypoxic incubator (1% O_2, 5% CO_2, 94% N_2) for 6 h. Other procedures were similar to normoxic conditions except that cells were incubated in hypoxia.

1.20 Investigation of lipid peroxidation *in vitro*

Hepa1-6 cells were seeded into 12-well plates and allowed to finish cell adherence. The media were then replaced with fresh culture media containing 10 μM **HTQ-Fc** and incubated for 24 h. And then the media were replaced with 2 μM C11-BODIPY$^{TM\ 589/591}$ for 30 min incubation. After washing with PBS, the fluorescence images were taken immediately by the fluorescence inverted microscope. For the irradiation group, the

cells were irradiated with white light (60 mW cm^{-2}) for 15 min after incubation with 2 μM C11-BODIPY$^{TM\ 589/591}$.

1.21 Evaluation of Caspase 3 activity in cells

Strict operating procedures were performed based on the Caspase 3 Activity Assay Kit (Beyotime) instructions.

1.22 Evaluation of GSH levels in cells

Strict operating procedures were carried out according to the instructions of GSH and GSSG Assay Kit (Beyotime).

1.23 Animal model and *in vivo* imaging

All the animal experiments were conducted in accordance with the protocols approved by the animal ethics committee of Central South University (Changsha, China), and performed in compliance with institutional guidelines for animal welfare. Female C57BL/6J mice and BALB/c nude mice, 4 weeks, were obtained from the Laboratory Animal Center of Central South University. The mice were housed under a 12 h light/dark cycle and allowed free access to food and water.

APAP-induced liver injury mouse model. The BALB/c nude mice were randomly divided into three groups: the APAP-induced group, the NAC-remediated group, and the Saline group. Before the experiment, the mice fasted overnight. For the APAP-induced group, saline (100 μL) was administered *via* intraperitoneal injection, followed by N-acetyl-p-aminophenol (APAP, 300 mg/kg, 300 μL) injected intraperitoneally after 2 h. The mice were then treated with **HTQ** (100 μM, 100 μL) or **HTQ-Fc** (100 μM, 100 μL) *via* intraperitoneal injection after an additional 10 h. For the NAC-remediated group, N-acetylcysteine (NAC, 300 mg/kg, 100 μL) was administered intraperitoneally instead of saline, followed by the same APAP and **HTQ**/**HTQ-Fc** treatment protocol as the APAP-induced group. For the Saline group, 300 μL saline was administered intraperitoneally instead of APAP, with other procedures consistent with the APAP-induced group. All mice were euthanized after a total experimental duration of 14 h to harvest the major organs for *ex vivo* fluorescence imaging using the S12-IVIS SPERTRUM living imaging system. Excitation filter: 465 nm, Emission filter: 700 nm, Exposure: 50 s.

Hepa1-6 tumor-bearing mouse model. Hepa1-6 cells (1×10^7 cells) were subcutaneously inoculated into the right axillary region of the C57BL/6J mice or BALB/c nude mice. The tumor volume of the mice was calculated as volume $A = a * b^2/2$ (a: length; b: width). Tumor xenograft BALB/c nude mice were given **HTQ** (100 μM, 100 μL) or **HTQ-Fc** (100 μM, 100 μL) by intratumoral injection during mouse anesthesia. *In vivo* fluorescence images were taken by the S12-IVIS SPERTRUM living imaging system at different time points. Excitation filter: 465 nm, Emission filter: 700 nm, Exposure: 5 s.

1.24 *In vivo* antitumor effect

The antitumor efficacy of **HTQ** and **HTQ-Fc** was assessed in Hepa1-6 tumors bearing C57BL/6J mice (initially around 100 mm^3, Day 0). The mice were randomly divided into 6 groups (n = 5), including (1) intratumor injection of saline (100 μL) (Control); (2) intratumor injection of saline with irradiation (100 μL) (Control + L); (3) intratumor injection of **HTQ** (100 μM, 100 μL) (**HTQ**); (4) intratumor injection of **HTQ-Fc** (100 μM, 100 μL) (**HTQ-Fc**); (5) intratumor injection of **HTQ** (100 μM, 100 μL) with irradiation (**HTQ** + L). (6) intratumor injection of **HTQ-Fc** (100 μM, 100 μL) with irradiation (**HTQ-Fc** + L). Photoirradiation (150 mW cm^{-2}) was administered 2 h post-injection to groups 2, 5, and 6 for 15 min. The process of injection and irradiation was repeated on Day 2. Tumor dimensions and body weights were measured on alternate days from Day 0 to Day 10. On Day 10, mice in six groups were humanely euthanized. Major organs (heart, liver, spleen, lung, and kidney) and tumors were examined by H&E staining.

1.25 Hemolysis assay

Healthy mice blood (2 mL) was donated from female mice. RBCs were collected by centrifugation at 1500 rpm for 5 min, washed with normal saline until the supernatant was clear, and resuspended using normal saline to prepare 2% erythrocyte solution. Then, different concentrations of **HTQ** or **HTQ-Fc** in normal saline solutions were added to the same volume of 2% erythrocyte solution in centrifuge tubes. After incubation at 37 °C for 2 h, the supernatant was obtained through centrifugation at 2500 rpm for 5 min and transferred to a 96-well plate. The absorbance at 540 nm was

measured by a microplate reader. RBCs in normal saline and deionized water were used as a negative control and a positive control, respectively. The following formula was used to calculate the hemolysis percentage: Hemolysis (%) = (sample absorbance - negative control absorbance) / (positive control absorbance - negative control absorbance) × 100.

2. Figures

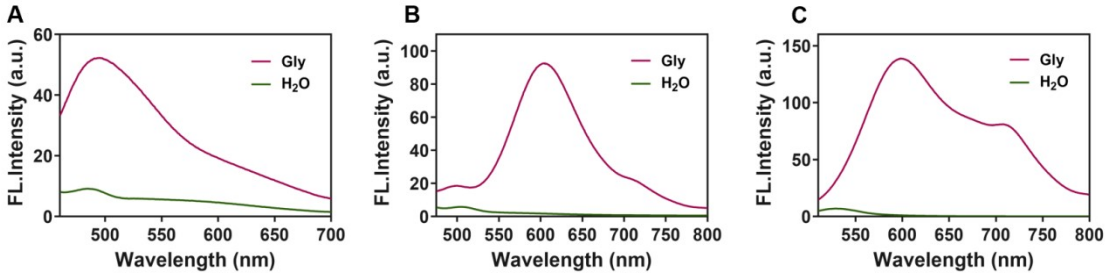

Figure S1. Fluorescence spectra of **HPQ** (A), **HFQ** (B), or **HTQ** (C) in water or glycerin. Concentration of probes: 10 μM.

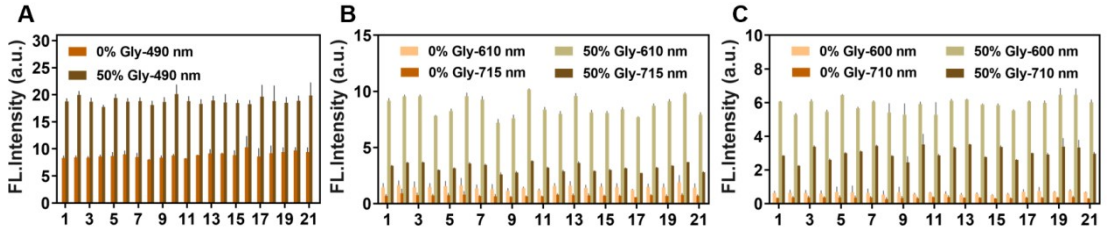

Figure S2. Fluorescence responses of **HPQ** (A), **HFQ** (B), or **HTQ** (C) for various analytes. Analytes (100 μM): 1, only probe; 2, $Zn(OAc)_2$; 3, $FeSO_4$; 4, $CoCl_2$; 5, $CaCl_2$; 6, $MgSO_4$; 7, $AlCl_3$; 8, NaBr; 9, NaI; 10, KNO_3; 11, $NaNO_2$; 12, Na_2SO_3; 13, glucose; 14, galactose; 15, H_2O_2; 16, valine; 17, glycine; 18, proline; 19, cysteine; 20, glutamic acid; 21, leucine. Concentration of probes: 10 μM.

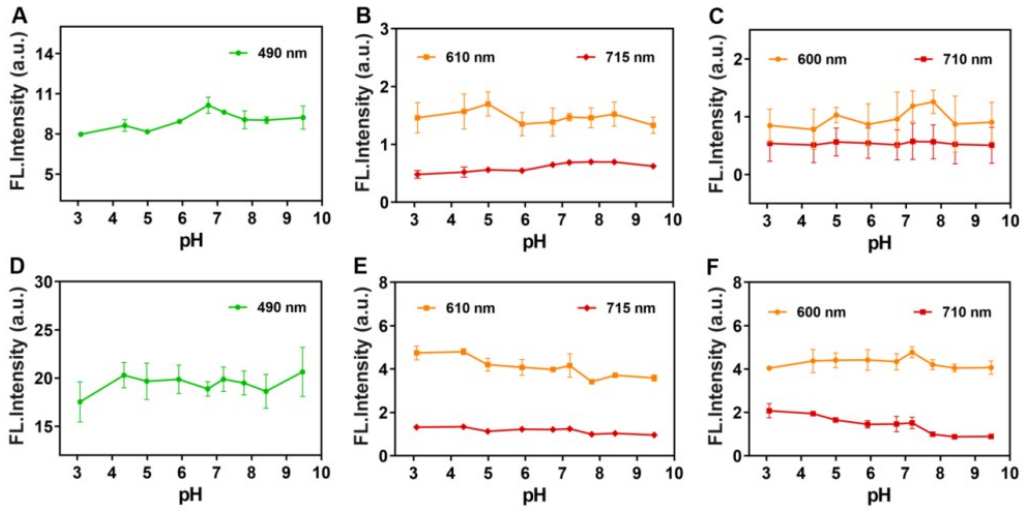

Figure S3. Fluorescence of **HPQ** (A), **HFQ** (B), or **HTQ** (C) at the emission peak in PBS with different pH values. Fluorescence of **HPQ** (D), **HFQ** (E), or **HTQ** (F) in PBS with different pH values containing 50% glycerin at the emission peak. **HPQ**, λ_{ex} = 420

nm. **HFQ**, λ_{ex} = 435 nm. **HTQ**, λ_{ex} = 460 nm. Concentration of probes: 10 μM.

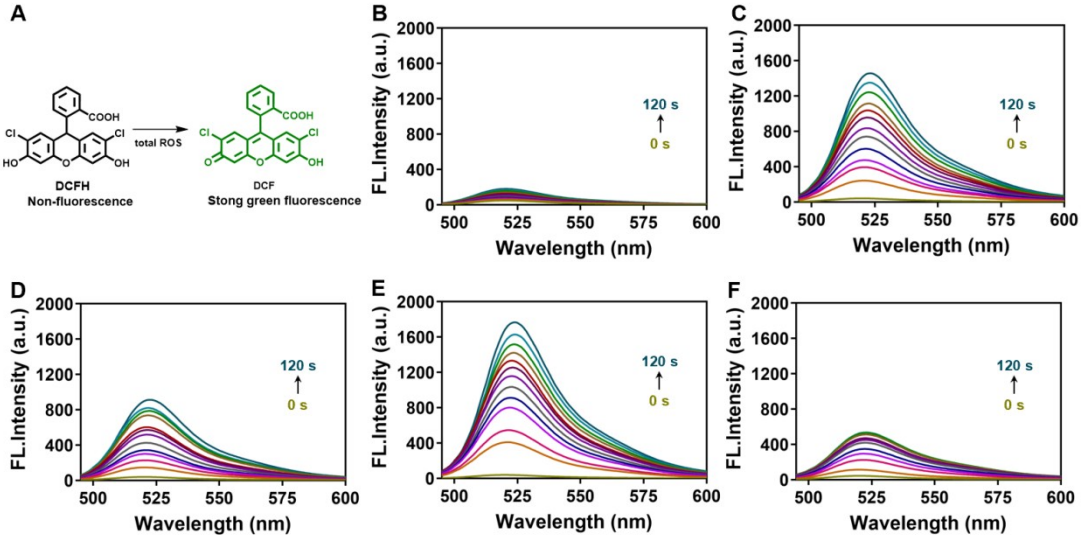

Figure S4. (A) Mechanism of DCFH for total ROS detection. (B) Fluorescence spectra of 50 μM DCFH upon various periods of white light irradiation (60 mW cm^{-2}). Fluorescence spectra of 50 μM DCFH with **HPQ** (C) or **HFQ** (D) or **HTQ** (E) or Ce6 (F) upon various periods of white light irradiation (60 mW cm^{-2}). Concentration of photosensitizers: 10 μM.

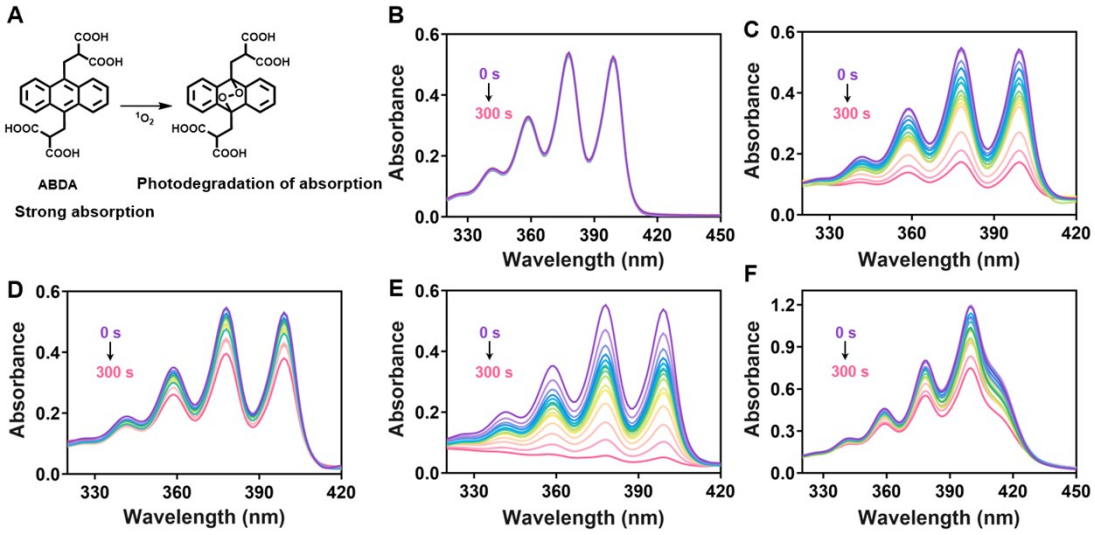

Figure S5. (A) Mechanism of ABDA for the detection of $^1O_2$. (B) UV-vis absorption spectra of 50 μM ABDA upon various periods of white light irradiation (60 mW cm^{-2}). UV-vis absorption spectra of 50 μM ABDA with **HPQ** (C) or **HFQ** (D) or **HTQ** (E) or Ce6 (F) upon various periods of white light irradiation (60 mW cm^{-2}). Concentration of

photosensitizers: 10 μM.

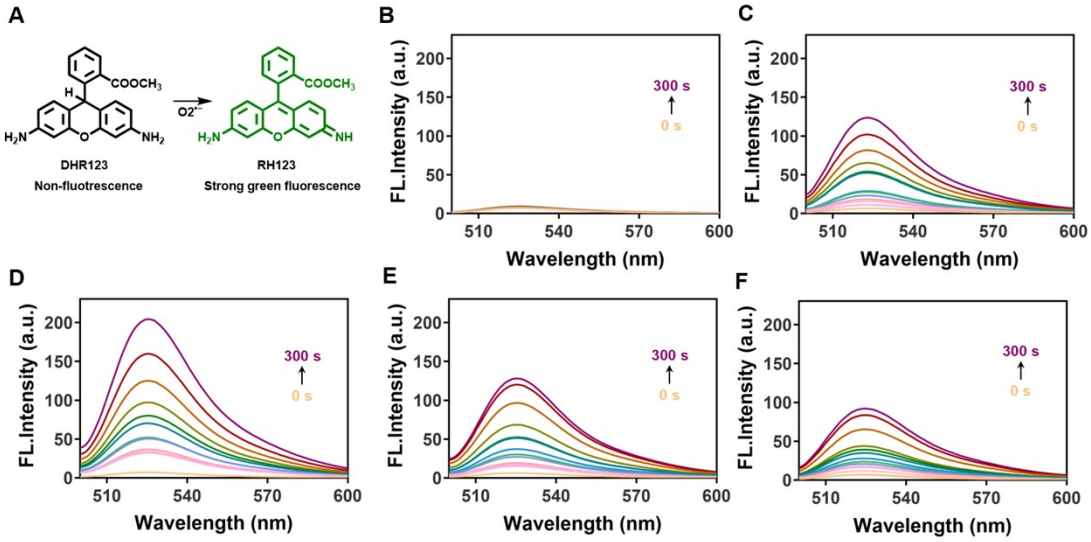

Figure S6. (A) Mechanism of DHR123 for $O_2^{\bullet-}$ detection. (B) Fluorescence spectra of 5 μM DHR123 upon various periods of white light irradiation (60 mW cm^{-2}). Fluorescence spectra of 5 μM DHR123 with **HPQ** (C) or **HFQ** (D) or **HTQ** (E) or Ce6 (F) upon various periods of white light irradiation (60 mW cm^{-2}). Concentration of photosensitizers: 10 μM.

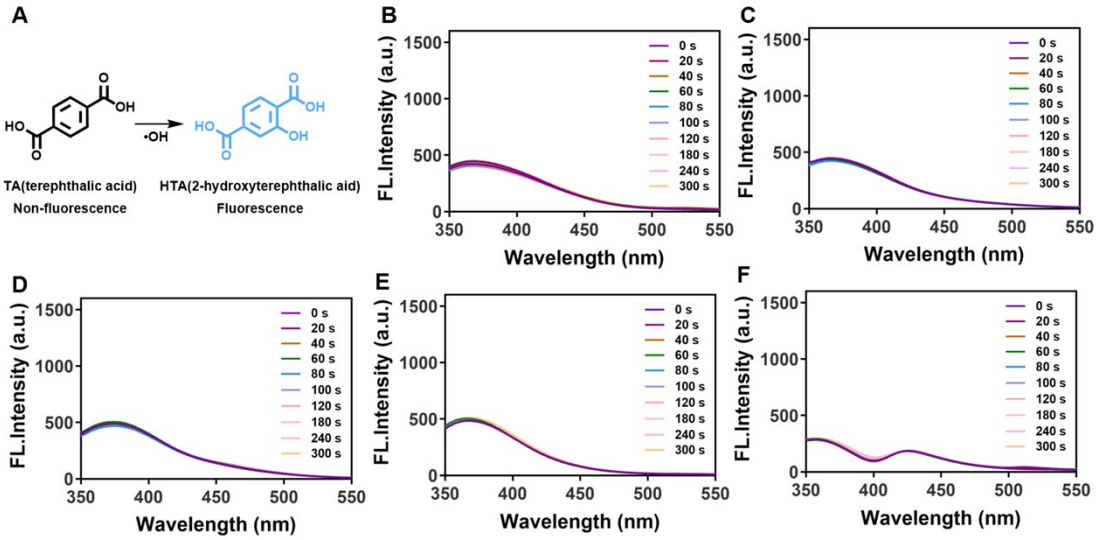

Figure S7. (A) Mechanism of TA for •OH detection. (B) Fluorescence spectra of 5 mM TA upon various periods of white light irradiation (60 mW cm^{-2}). Fluorescence spectra of 5 mM TA with **HPQ** (C) or **HFQ** (D) or **HTQ** (E) or Ce6 (F) upon various periods of white light irradiation (60 mW cm^{-2}). Concentration of photosensitizers: 10 μM.

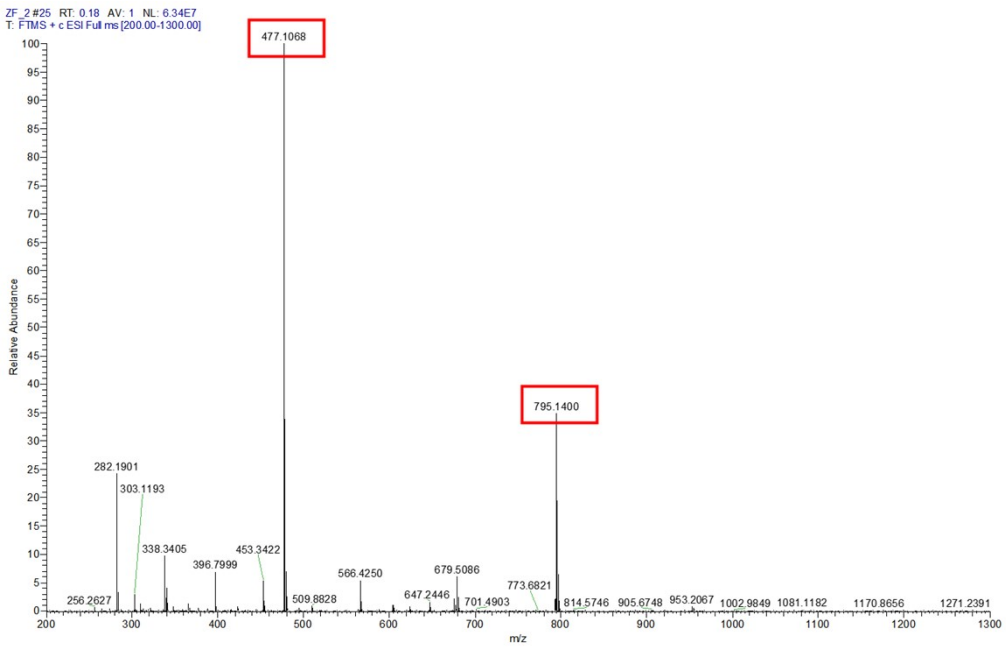

Figure S8. ESI-MS of the solution of 10 μM **HTQ-Fc** mixed with 2 U/mL CE.

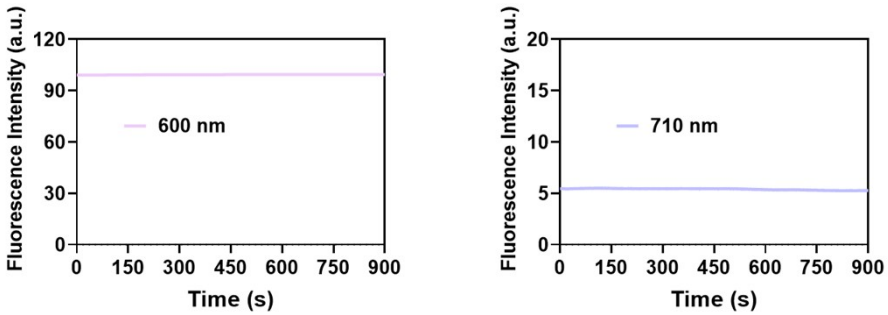

Figure S9. Photostability of **HTQ-Fc** (10 μM) at 600 nm (left) and 710 nm (right) in 50% glycerin/water solution under continuous irradiation. λ_{ex} = 470 nm.

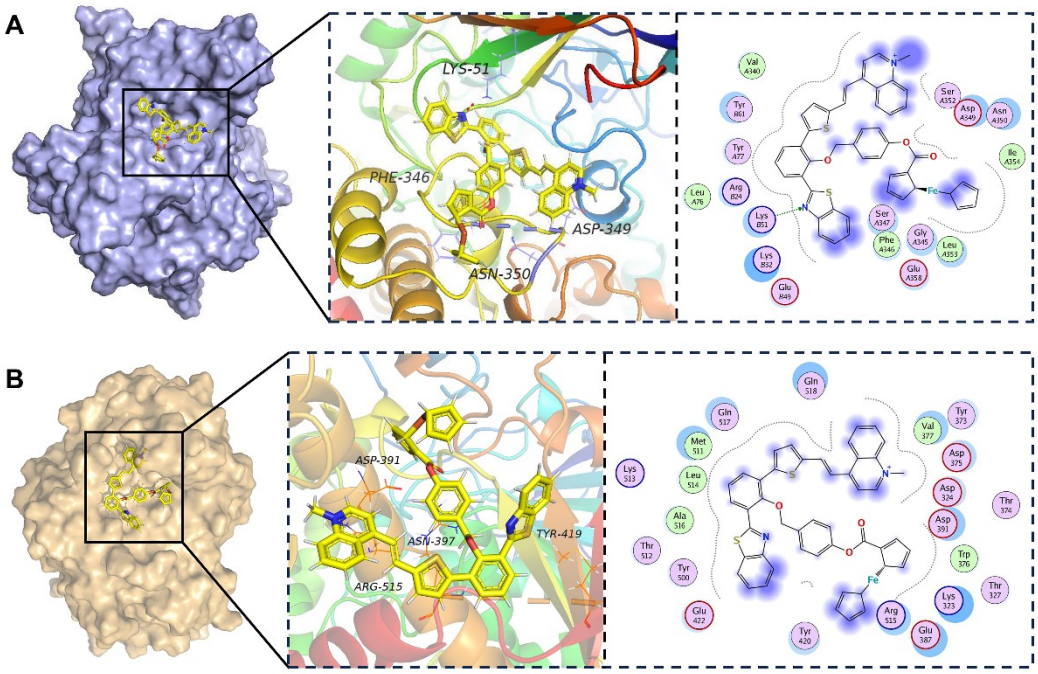

Figure S10. (A) Molecular analog docking plot of **HTQ-Fc** at AChE (PDB ID: 1B41). (B) Molecular analog docking plot of **HTQ-Fc** at BChE (PDB ID: 1P0M).

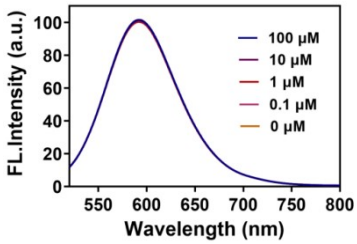

Figure S11. Effects of BNPP at varied concentrations on the fluorescence of **HTQ -Fc** (10 μM).

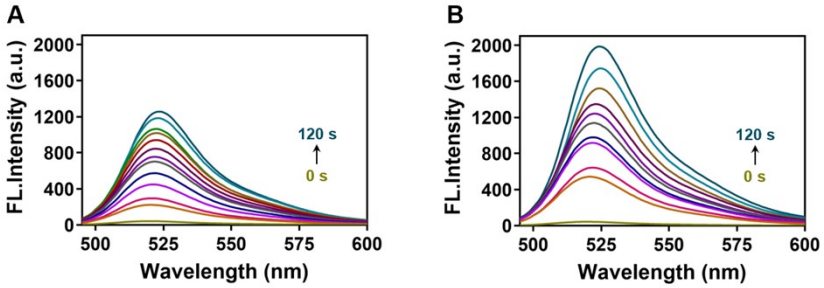

Figure S12. (A) FL spectra of 50 μM DCFH with 10 μM **HTQ-Fc** upon various periods of white light irradiation (60 mW cm^{-2}). (B) FL spectra of 50 μM DCFH with 10 μM **HTQ-Fc** (pretreated with 2 U/mL CE for 1 h) upon various periods of white light irradiation (60 mW cm^{-2}).

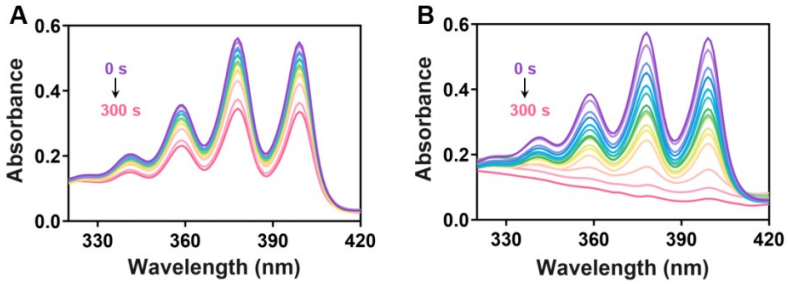

Figure S13. (A) UV-vis absorption spectra of 50 μM ABDA with 10 μM **HTQ-Fc** upon various periods of white light irradiation (60 mW cm^{-2}). (B) UV-vis absorption spectra of 50 μM ABDA with 10 μM **HTQ-Fc** (pretreated with 2 U/mL CE for 1 h) upon various periods of white light irradiation (60 mW cm^{-2}).

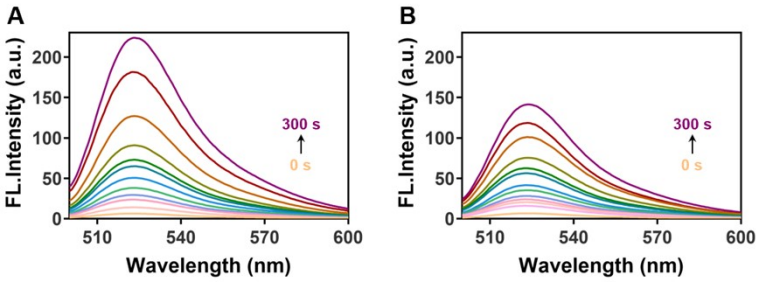

Figure S14. (A) FL spectra of 5 μM DHR123 with 10 μM **HTQ-Fc** upon various periods of white light irradiation (60 mW cm^{-2}). (B) FL spectra of 5 μM DHR123 with 10 μM **HTQ-Fc** (pretreated with 2 U/mL CE for 1 h) upon various periods of white light irradiation (60 mW cm^{-2}).

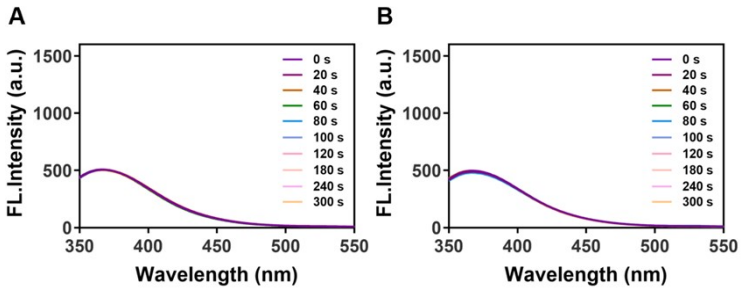

Figure S15. (A) FL spectra of 5 mM TA with 10 μM **HTQ-Fc** upon various periods of white light irradiation (60 mW cm^{-2}). (B) FL spectra of 5 mM TA with 10 μM **HTQ-Fc** (pretreated with 2 U/mL CE for 1 h) upon various periods of white light irradiation (60 mW cm^{-2}).

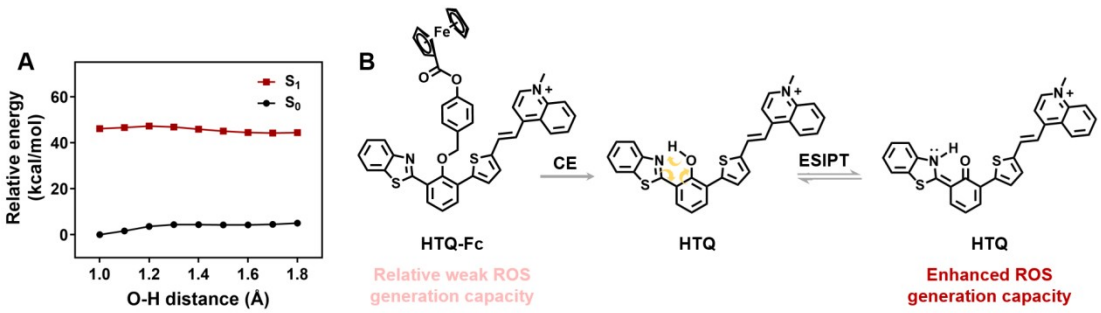

Figure S16. (A) CAM-B3LYP/def2-SVP optimized the S energy profiles along the O-H distances in the enol form of **HTQ**. (B) Schematic illustration of the formation of the keto form of **HTQ** *via* ESIPT process after **HTQ-Fc** response to CE.

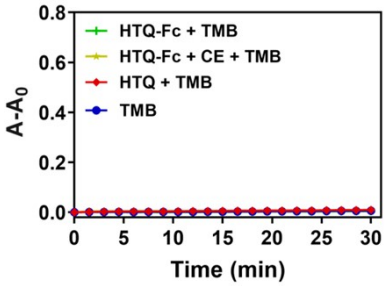

Figure S17. Changes of absorption intensity of different TMB solutions at 652 nm for different times.

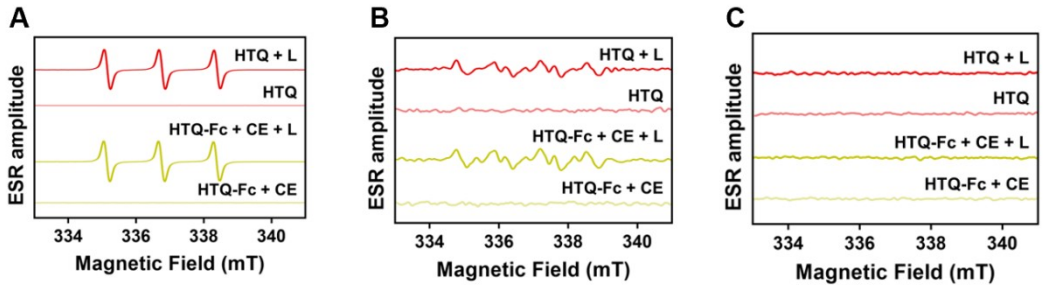

Figure S18. (A) ESR spectra of TEMP for $^1O_2$ characterization in different DMSO solutions with/without white light irradiation (60 mW cm^{-2}). (B) ESR spectra of DMPO for $O_2^{\bullet-}$ characterization in different DMSO solutions with/without white light irradiation (60 mW cm^{-2}). (C) ESR spectra of DMPO for •OH characterization in different PBS solutions with/without white light irradiation (60 mW cm^{-2}).

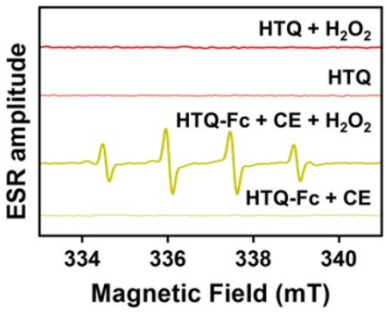

Figure S19. ESR spectra of DMPO for •OH characterization in different PBS solutions with/without H_2O_2.

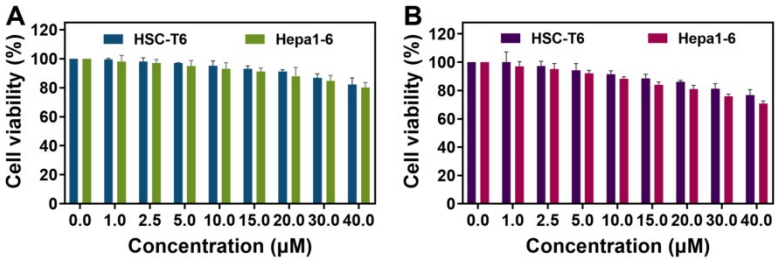

Figure S20. Cytotoxicity examination for different concentrations of **HTQ** (A) or **HTQ-Fc** (B) in HSC-T6 cells or Hepa1-6 cells.

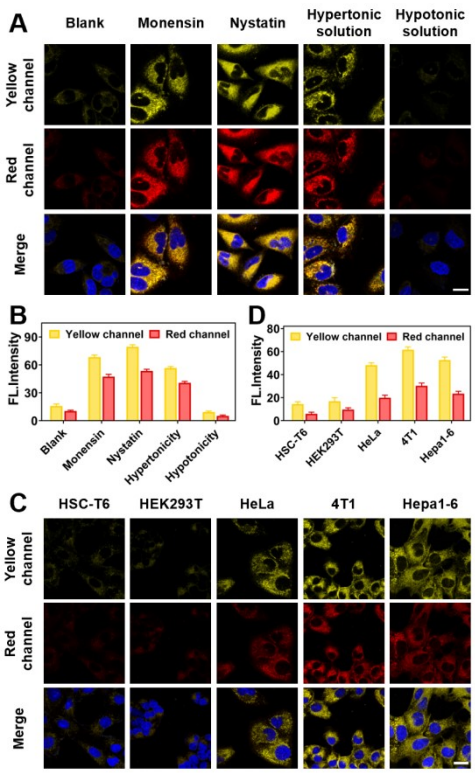

Figure S21. Monitoring intracellular viscosity by **HTQ** (10 μM). (A) CLSM images of

HeLa cells with different treatments. Scale bar: 20 μm. (B) Relative fluorescence intensity for panel A. (C) CLSM images of **HTQ** incubated in HSC-T6, HEK293T, HeLa, 4T1, or Hepa1-6 cells for 30 min. (D) Relative fluorescence intensity for panel C. Yellow channel: λ_{em} = 600 ± 20 nm, λ_{ex} = 470 nm. Red channel: λ_{em} = 710 ± 20 nm, λ_{ex} = 470 nm.

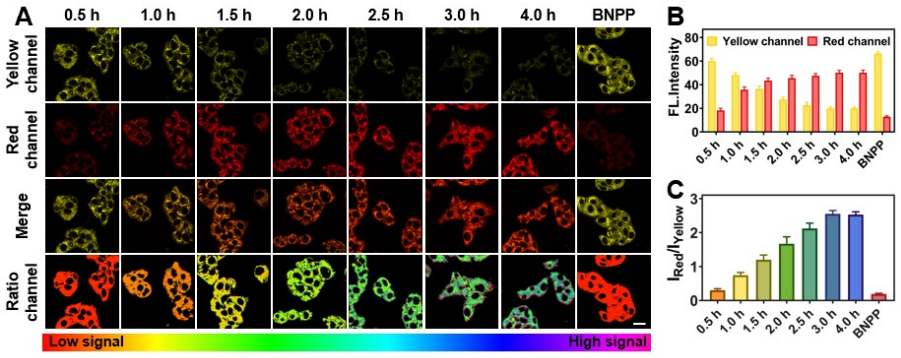

Figure S22. Fluorescence imaging of the intracellular CE by **HTQ-Fc** (10 μM). (A) CLSM images of HepG2 cells incubated with 10 μM **HTQ-Fc** at different time points. The 8th column: the cells were pretreated with 1 mM BNPP for 1 h, and then incubated with the probe for 4 h. (B) Relative fluorescence intensity for panel A. (C) The intensity ratio of the red channel to the yellow channel for panel A. Yellow channel: λ_{em} = 600 ± 20 nm, λ_{ex} = 470 nm. Red channel: λ_{em} = 710 ± 20 nm, λ_{ex} = 470 nm. Scale bar: 20 μm.

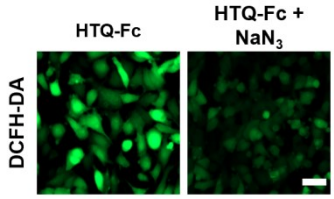

Figure S23. Evaluation of total ROS production with various treatments utilizing 5 μM DCFH-DA. Scale bars: 50 μm.

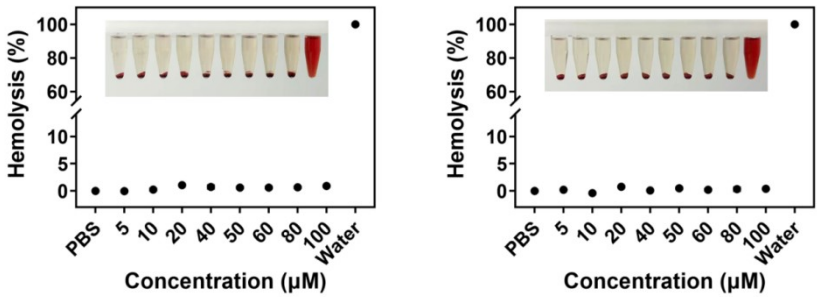

Figure S24. Hemolysis tests of **HTQ** (Left) and **HTQ-Fc** (Right). The inset photo was the solutions of the corresponding concentrations of the photosensitizer.

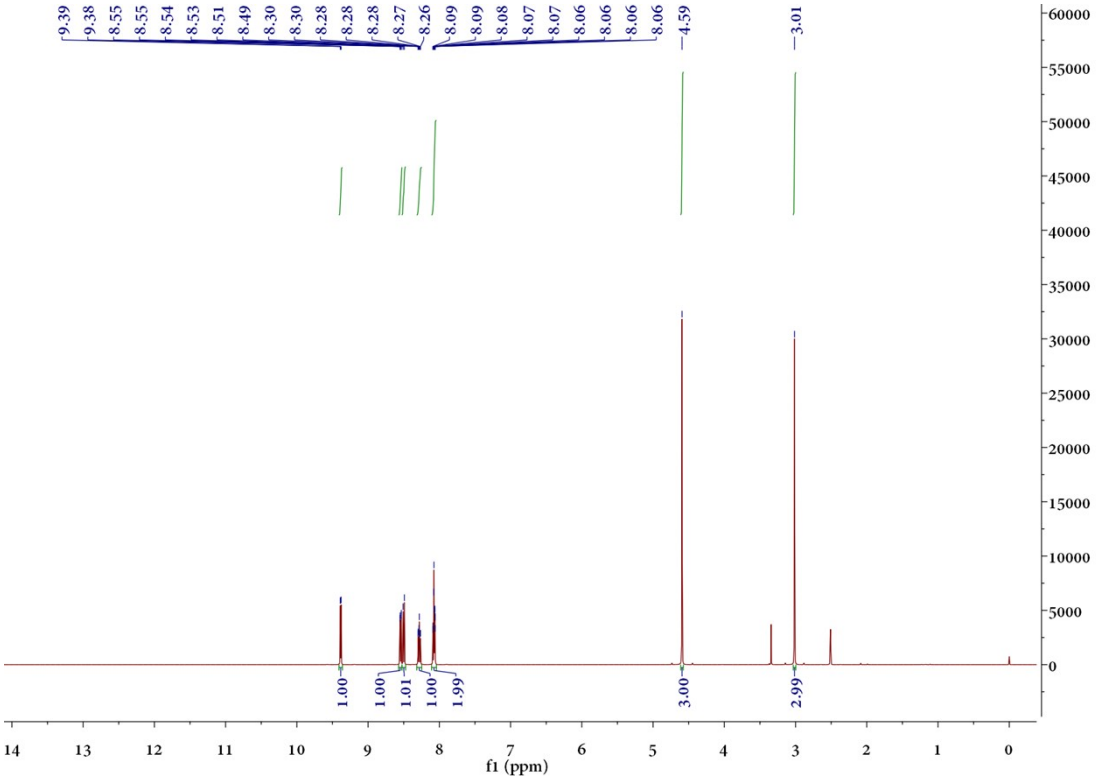

Figure S25. ^{1}H NMR spectrum of **Qu-C** in DMSO-d_6.

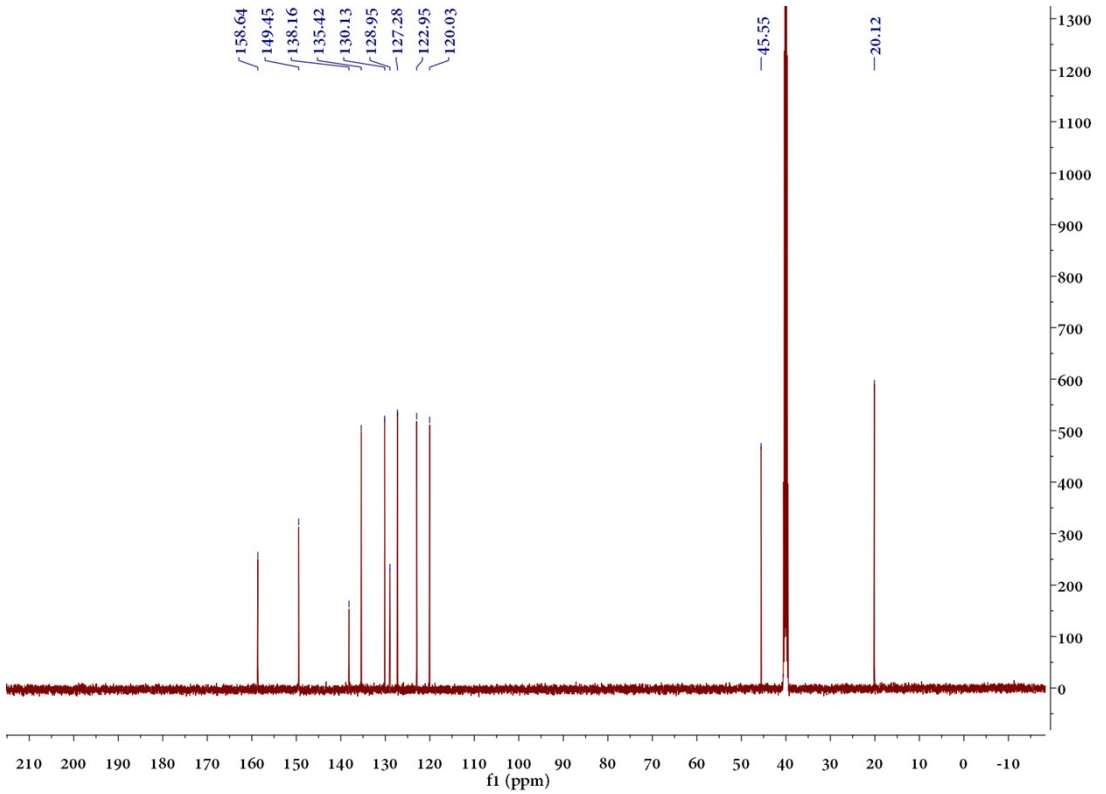

Figure S26. ^{13}C NMR spectrum of **Qu-C** in DMSO-d_6.

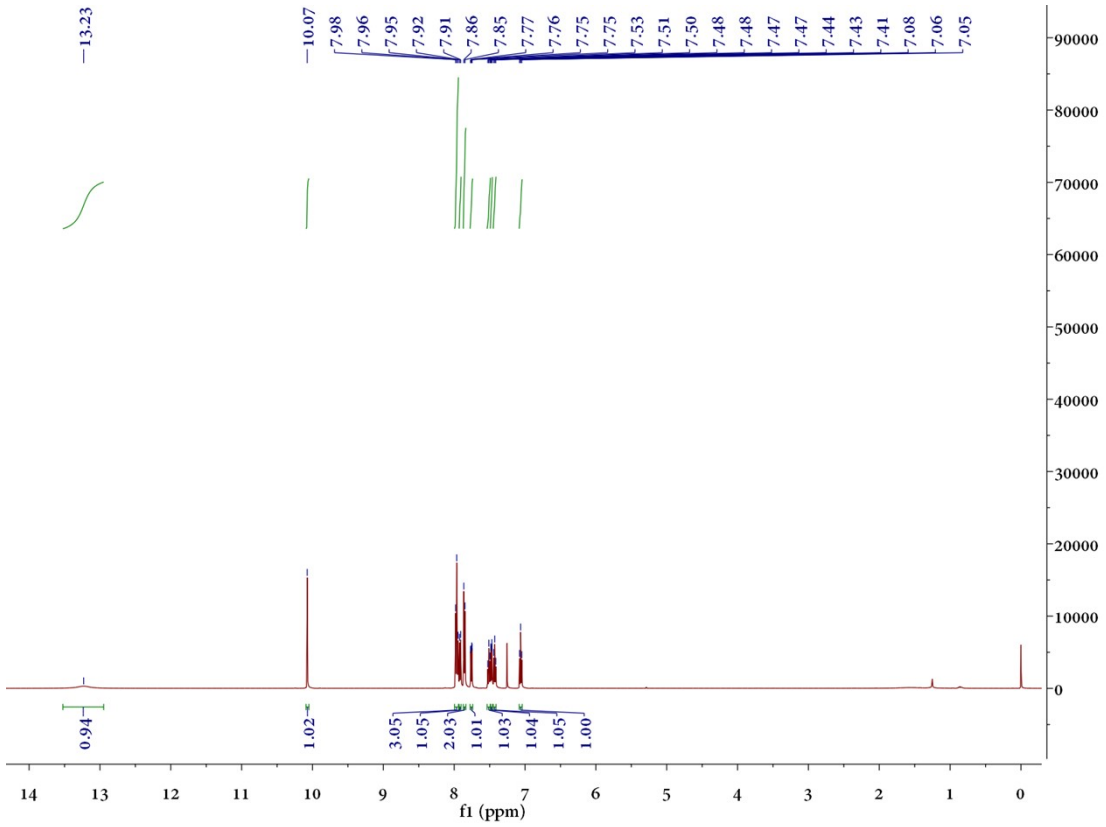

Figure S27. ^{1}H NMR spectrum of **HP-CHO** in $CDCl_3$.

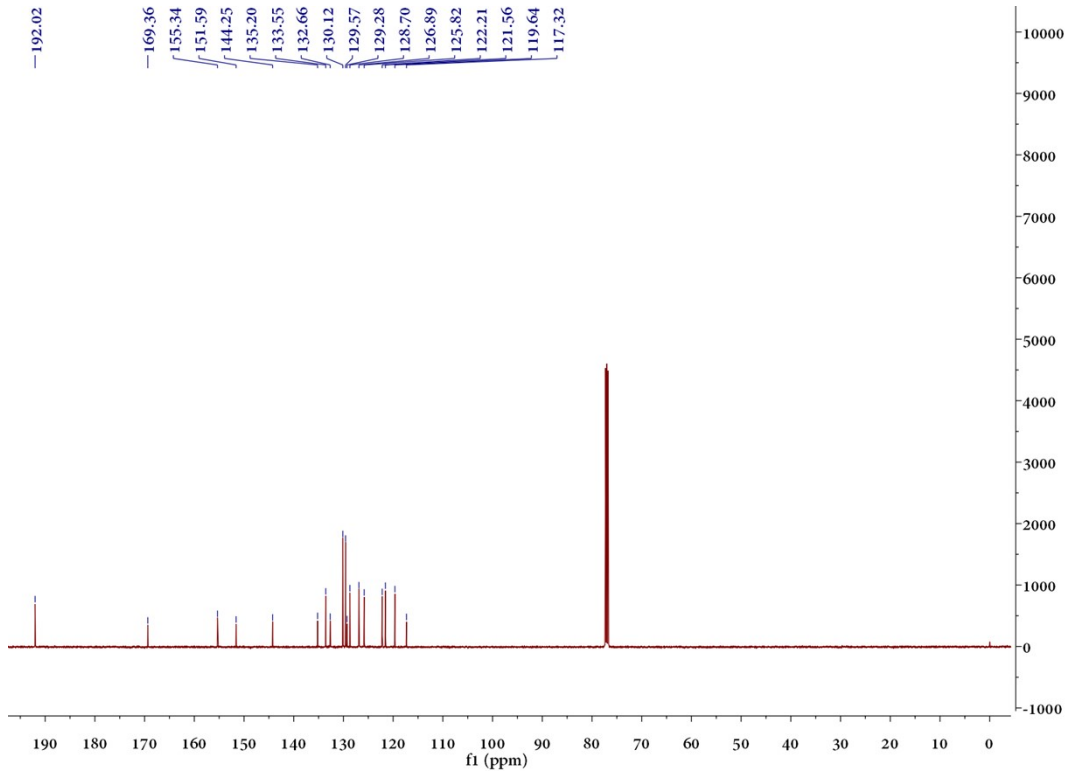

Figure S28. ^{13}C NMR spectrum of **HP-CHO** in $CDCl_3$.

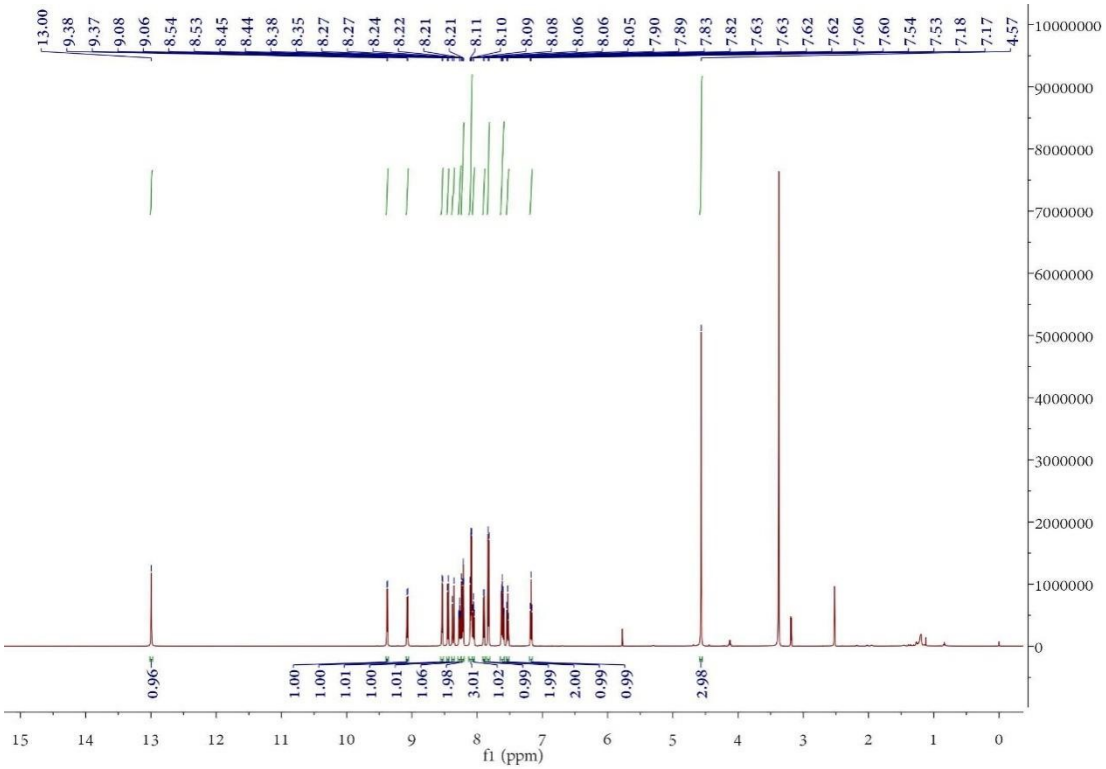

Figure S29. ^{1}H NMR spectrum of **HPQ** in DMSO-d_6.

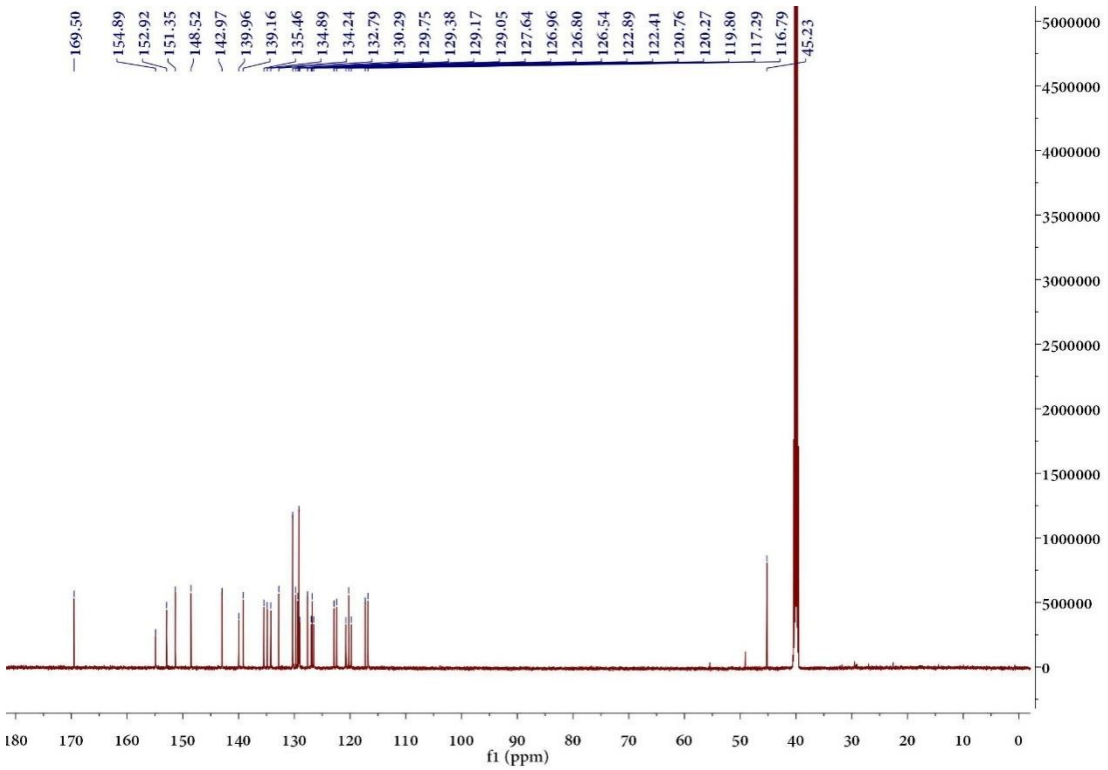

Figure S30. ^{13}C NMR spectrum of **HPQ** in DMSO-d_6.

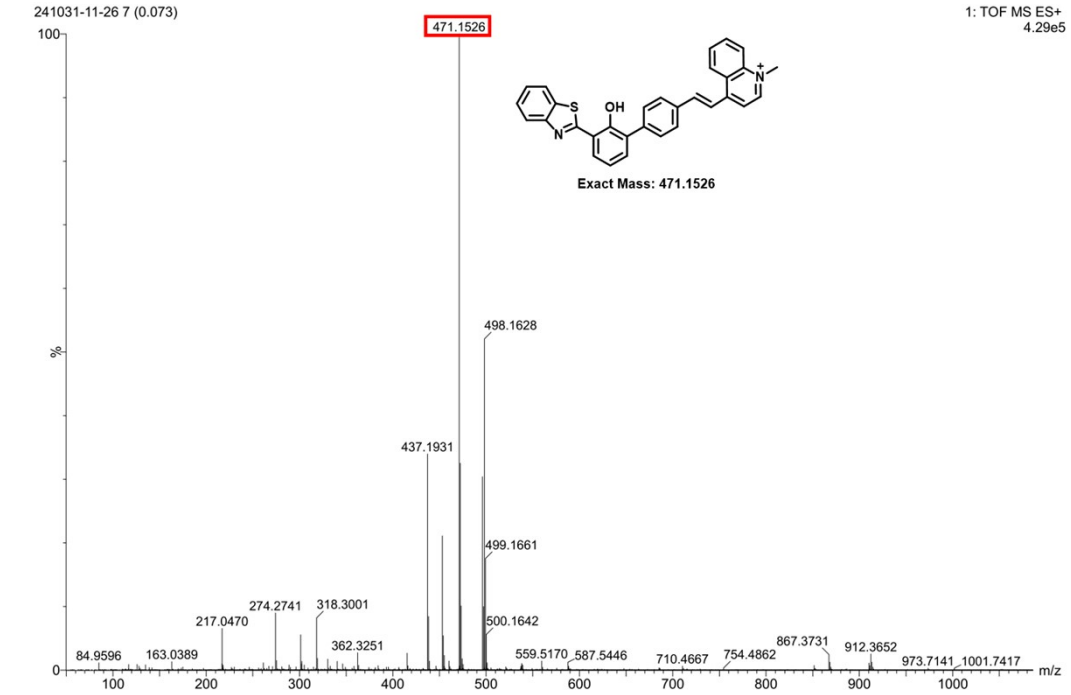

Figure S31. HRMS spectrum of **HPQ**.

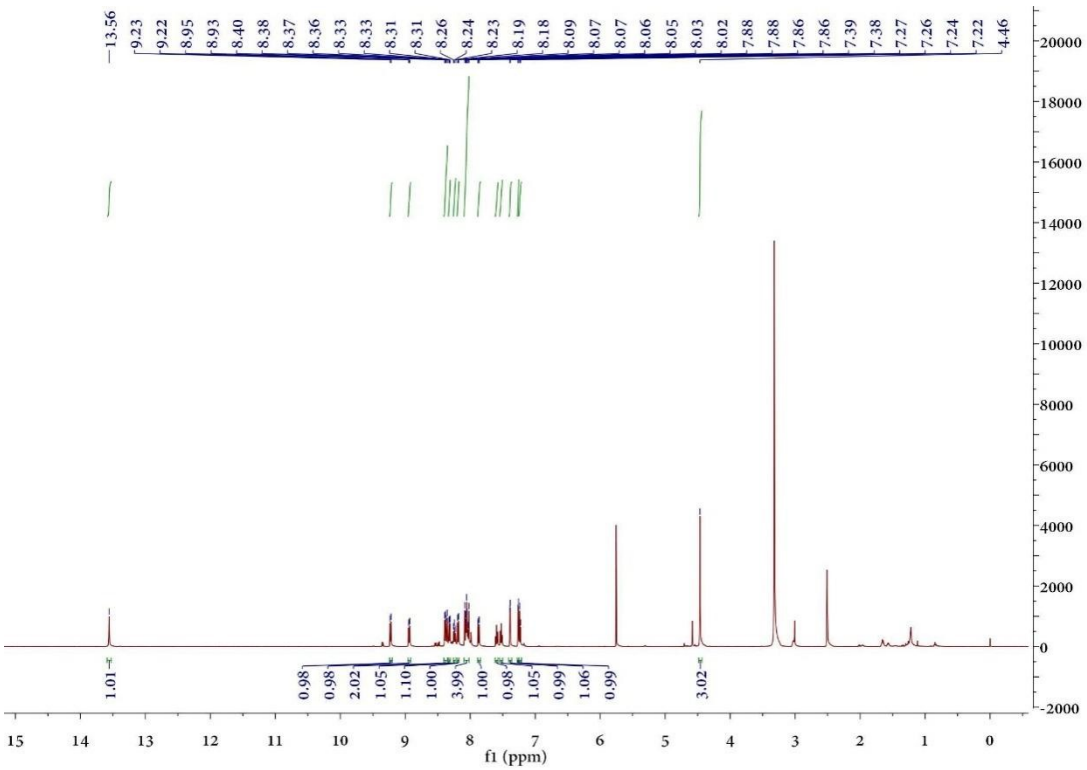

Figure S32. ^{1}H NMR spectrum of **HFQ** in DMSO-d_6.

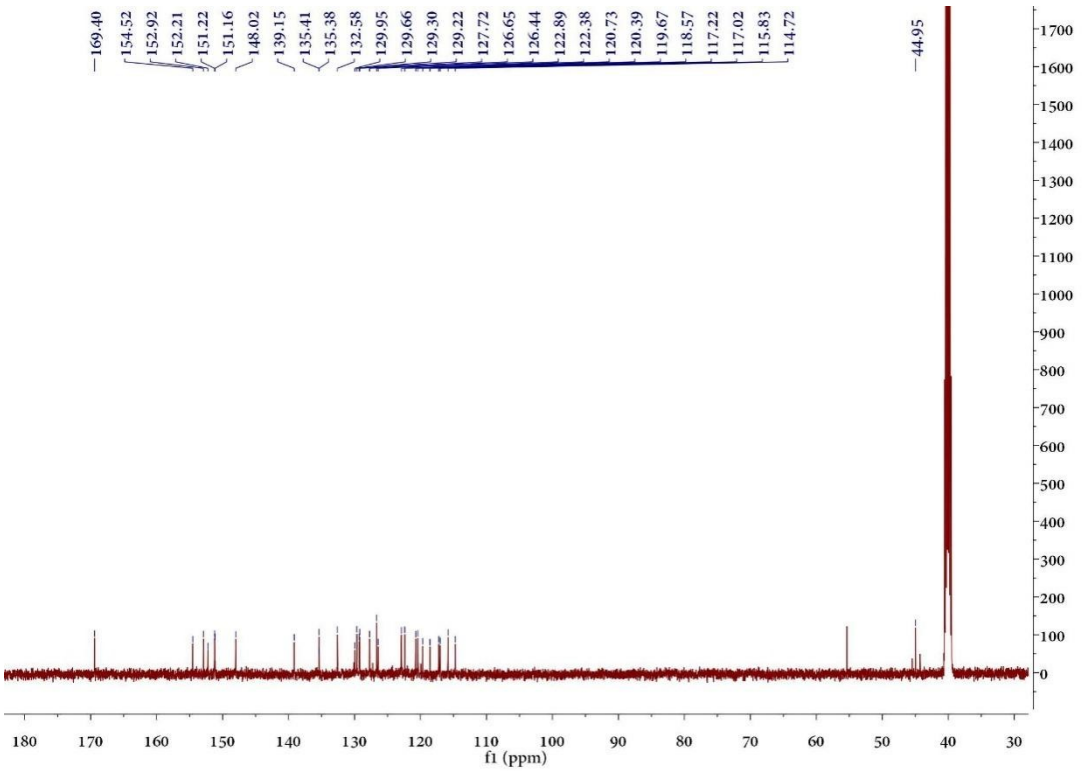

Figure S33. ^{13}C NMR spectrum of **HFQ** in DMSO-d_6.

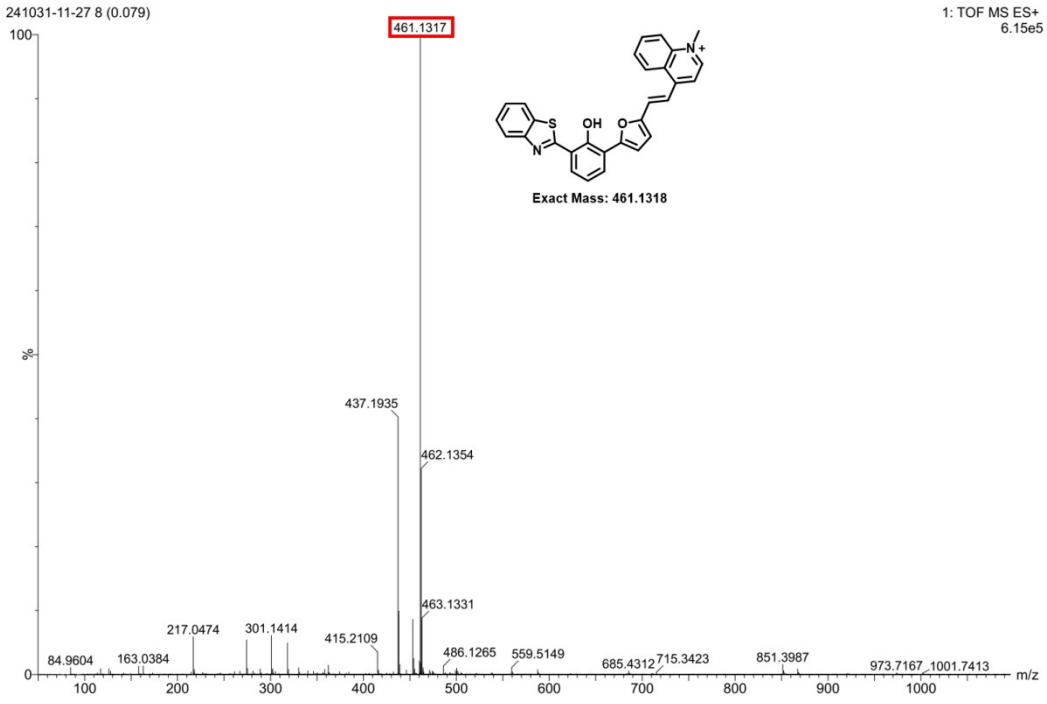

Figure S34. HRMS spectrum of **HFQ**.

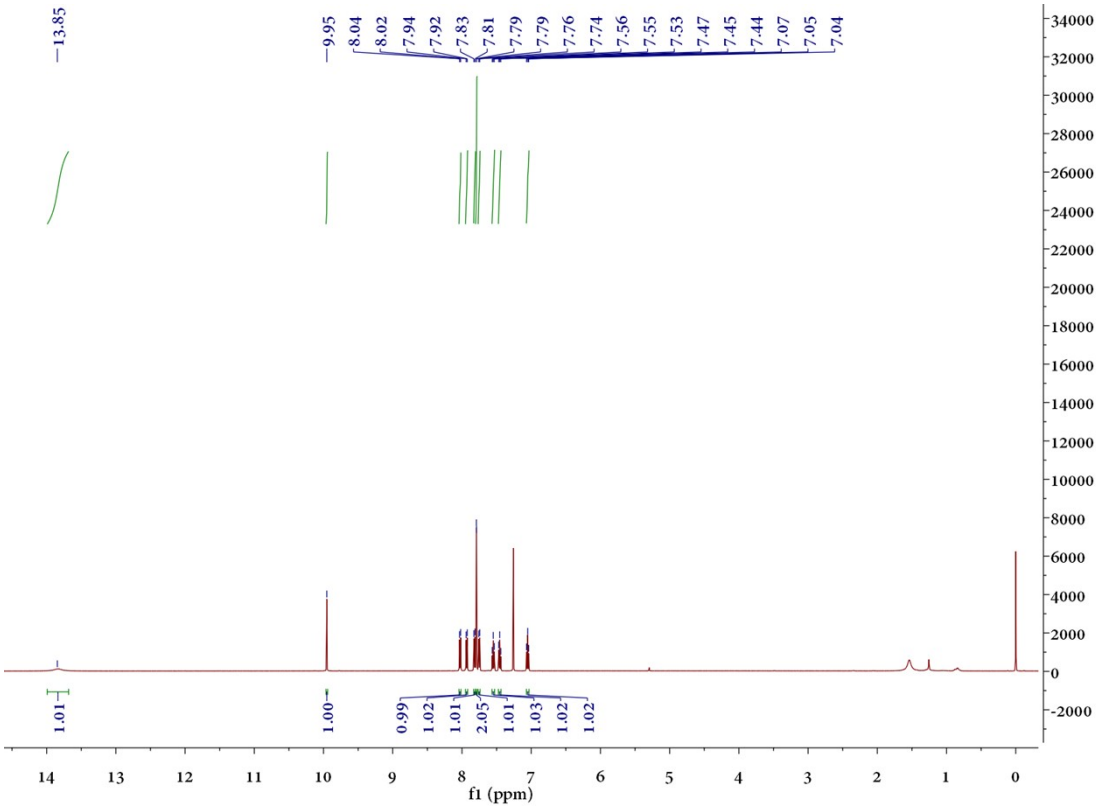

Figure S35. ^{1}H NMR spectrum of **HT-CHO** in $CDCl_3$.

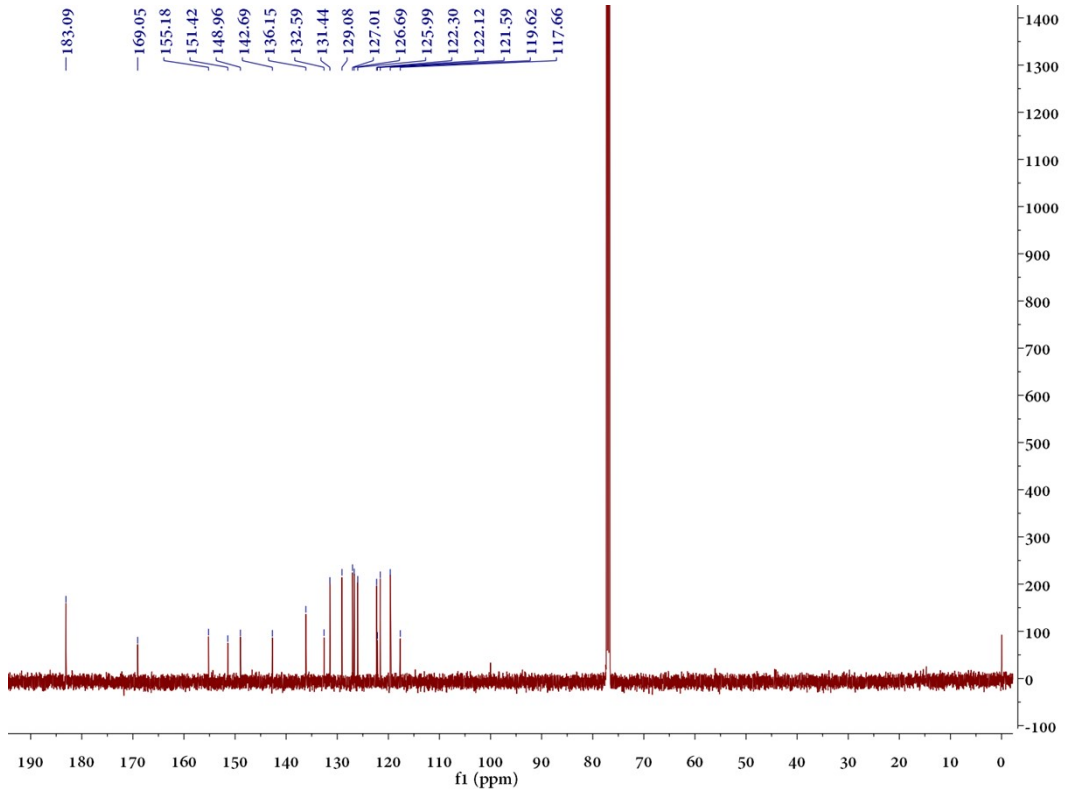

Figure S36. ^{13}C NMR spectrum of **HT-CHO** in $CDCl_3$.

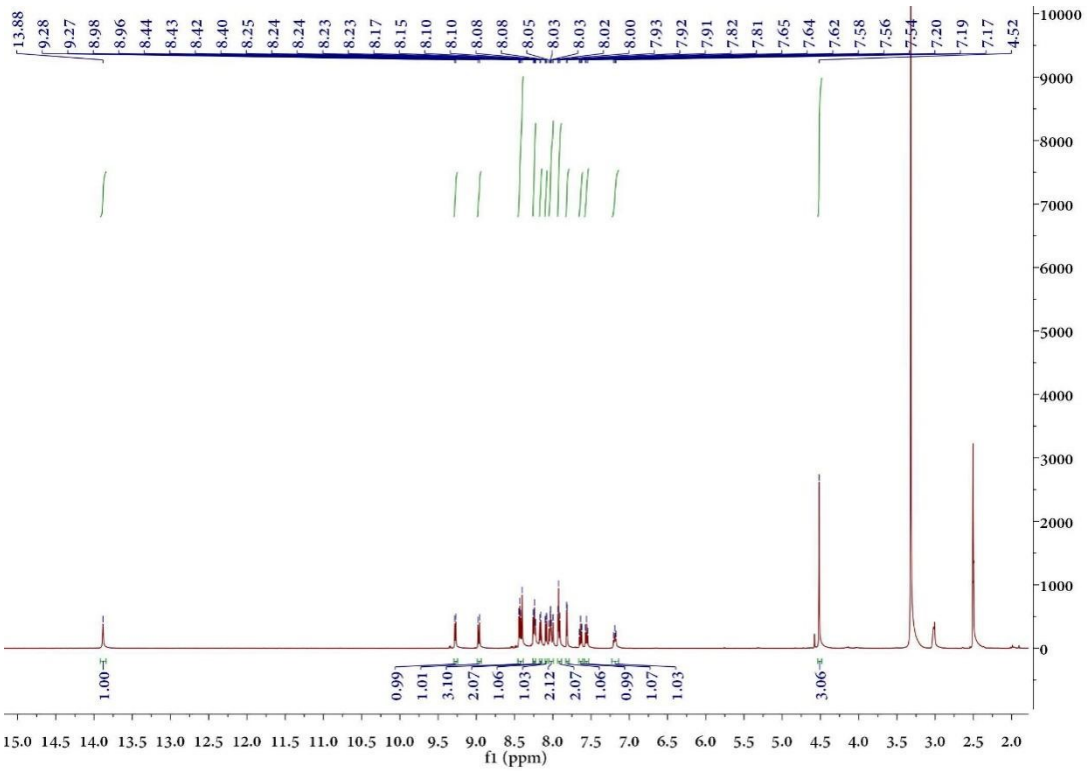

Figure S37. ^{1}H NMR spectrum of **HTQ** in DMSO-d_6.

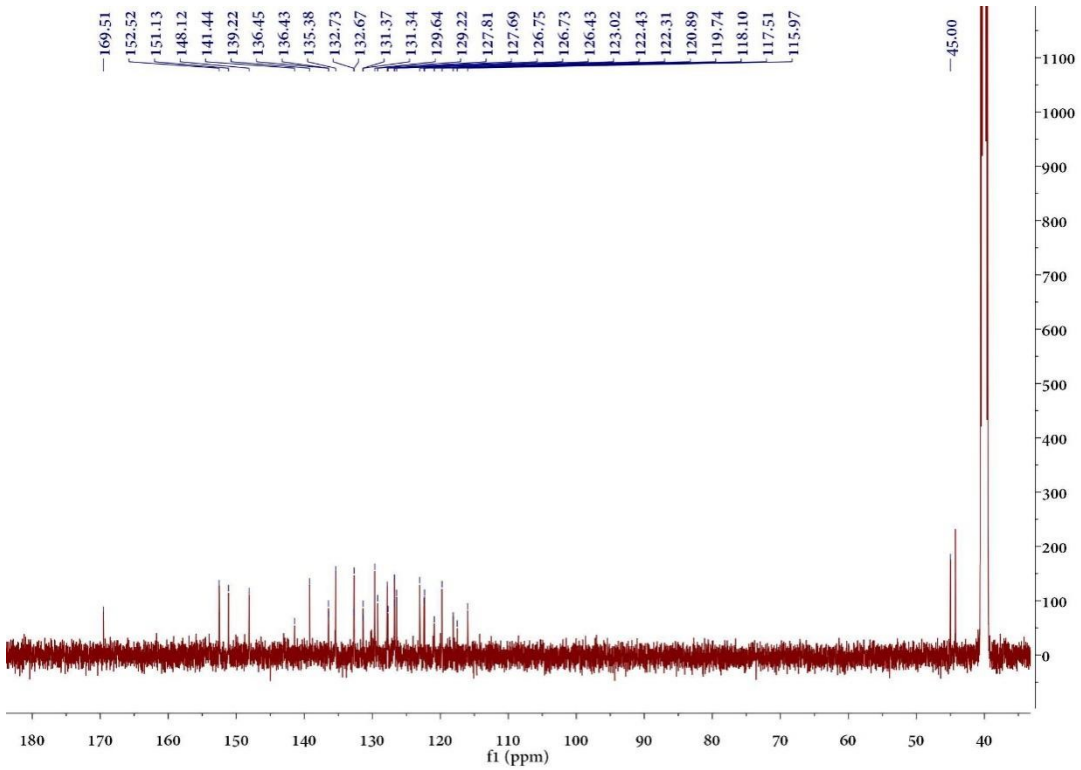

Figure S38. ^{13}C NMR spectrum of **HTQ** in DMSO-d_6.

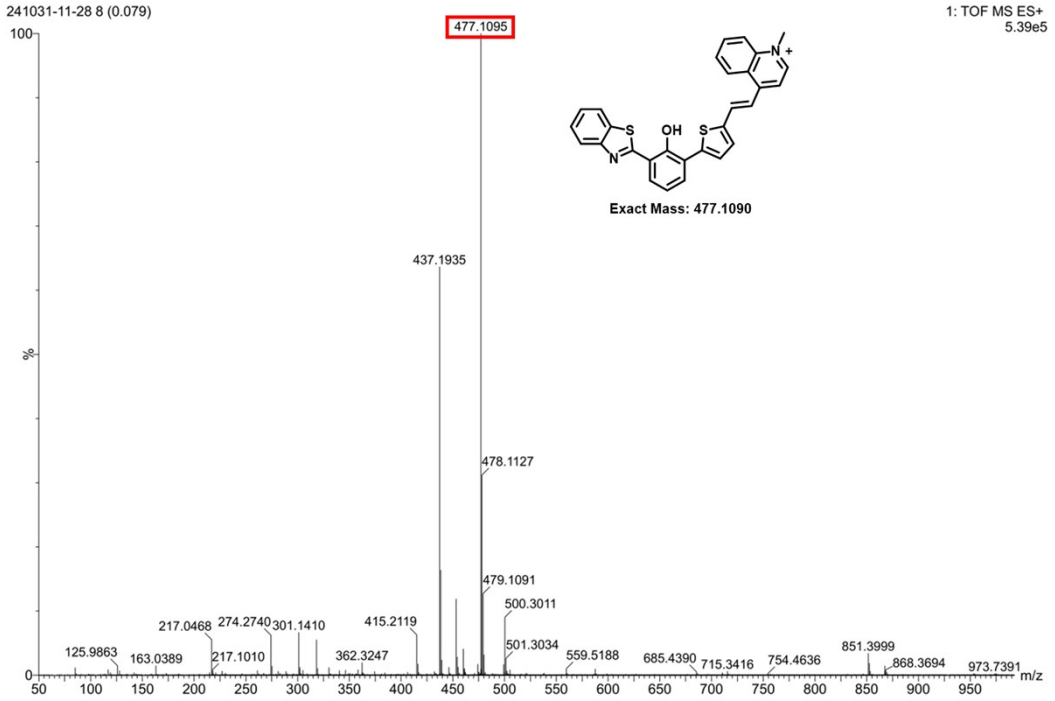

Figure S39. HRMS spectrum of **HTQ**.

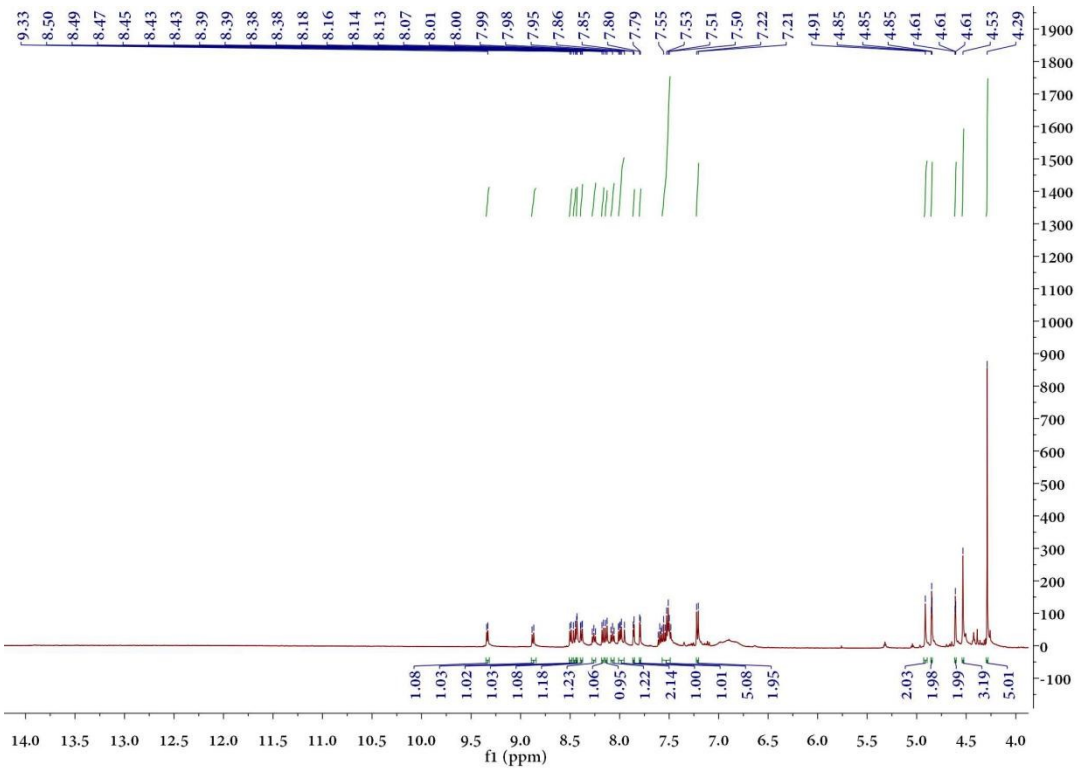

Figure S40. ^{1}H NMR spectrum of **HTQ-Fc** in DMSO-d_6.

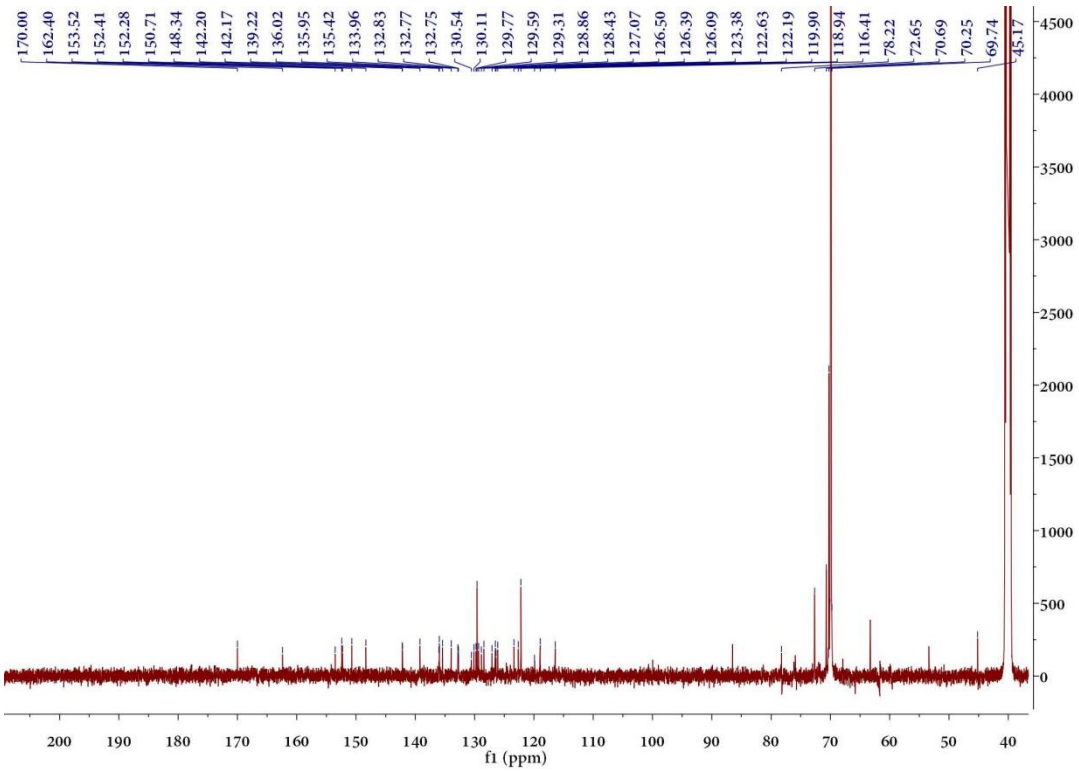

Figure S41. ^{13}C NMR spectrum of **HTQ-Fc** in DMSO-d_6.

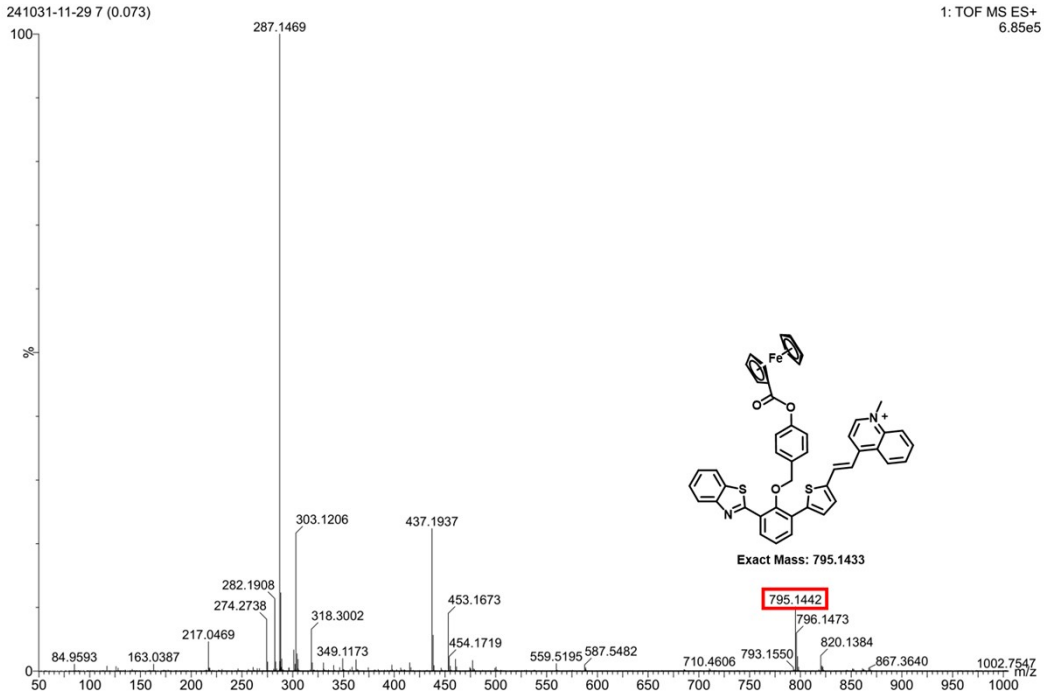

Figure S42. HRMS spectrum of **HTQ-Fc**.

3. Tables

Table S1. An overview on recently reported fluorescent probes for viscosity detection.

Probe	Solvent systems	$\lambda_{ex}/\lambda_{em}$ (nm)	Stokes shift (nm)	Degree of fluorescence enhancement	Applications	Reference
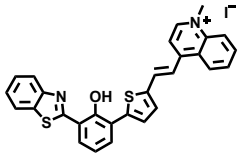	**Water/glycerin**	**460/600** **460/710**	**140** **250**	**249-fold** **319-fold**	**Specific imaging of HCC**	**This work**
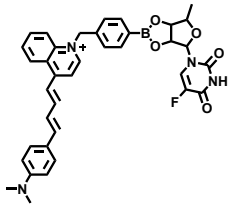	Water/glycerin	585/750	165	~ 38-fold	Cancer cells imaging	*Anal. Chem.,* 2025, 97, 2998-3008
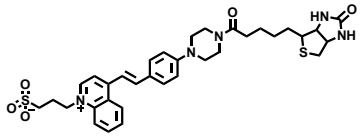	Water/glycerin	500/660	160	236-fold	Precise visualization of lung tumor	*Anal. Chem.,* 2025, 97, 1627-1634

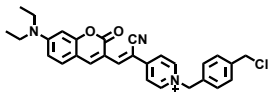	Water/glycerin	580/656	76	121-fold	Mitophagy visualization	*Biosens. Bioelectron.,* 2025, 276, 117246
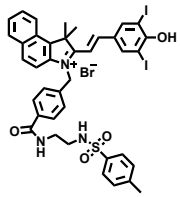	PBS/glycerin	580/620	40	163-fold	Diagnosis of nonalcoholic fatty liver and photodynamic cancer therapy	*Angew. Chem. Int. Ed.,* 2024, 63, e202316487
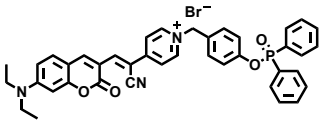	Water/glycerin	580/660	80	40-fold	Imaging of inflammation	*Biosens. Bioelectron.,* 2024, 254, 116233
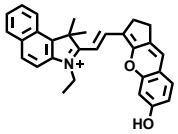	PBS/glycerin	680/737	57	21-fold	Tumor imaging and apoptosis monitoring	*Sens. Actuators B*, 2024, 418, 136247
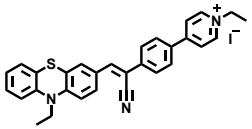	MeOH/glycerin	460/710	250	22-fold	Detection of atherosclerosis	*Chem. Eng. J.,* 2023, 464, 142687

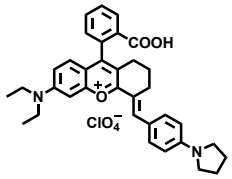	PBS/glycerin	649/740	91	~200-fold	Visualization of fatty liver	*Chem. Eng. J.,* 2022, 445, 136448
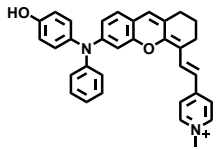	Water/glycerin	565/720	155	157-fold	Visualization of fatty liver, inflammation and photodynamic therapy	*Chem. Eng. J.,* 2022, 449, 137762
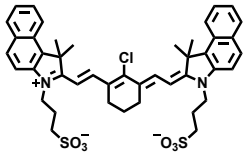	Water/glycerin	808/864	56	13-fold	Precision navigation of hepatic ischemia	*J. Am. Chem. Soc.,* 2022, 144, 30, 13586-13599
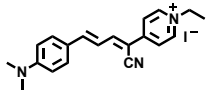	Water/glycerin	530/685	155	44-fold	Visualization of fatty liver	*Anal. Chem.,* 2021, 93, 9244-9249
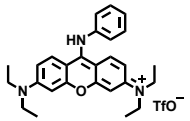	Water/glycerin	460/550	90	50-fold	Cancer visualization	*Anal. Chem.,* 2021, 93, 1786-1791
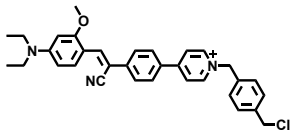	Water/glycerin	470/650	180	~ 92-fold	Real-time mitophagy monitoring	*Anal. Chem.,* 2021, 93, 3241-3249

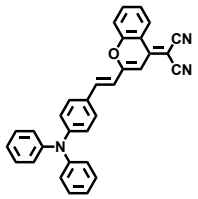	MeOH/glycerin	520/696	176	~ 30-fold	Noninvasive cancer diagnosis	*Anal. Chem.,* 2021, 93, 2072-2081
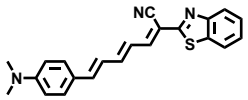	MeOH/glycerin	620/723	103	21-fold	Ferroptosis imaging	*ACS Sens.,* 2021, 6, 22−26

Table S2. The proportion of the CT state and the LE state in the S states or the T states.

	HTQ-Fc		**HTQ**	
	CT	LE	CT	LE
S	10.61%	89.39%	10.02%	89.98%
T	0.33%	99.67%	2.73%	97.27%
	ΔCT = 10.28%		ΔCT = 7.29%	